EUKARYOTIC CELL, Feb. 2007, p. 302–316 Vol. 6, No. 2
1535-9778/07/$08.00+0 doi:10.1128/EC.00321-06

GAS2 and *GAS4*, a Pair of Developmentally Regulated Genes Required for Spore Wall Assembly in *Saccharomyces cerevisiae*▽

Enrico Ragni,[1] Alison Coluccio,[2] Eleonora Rolli,[1] José Manuel Rodriguez-Peña,[3] Gaia Colasante,[1]† Javier Arroyo,[3] Aaron M. Neiman,[2] and Laura Popolo[1]*

Dipartimento di Scienze Biomolecolari e Biotecnologie, Università degli Studi di Milano, 20133 Milano, Italy[1]; Department of Biochemistry and Cell Biology, SUNY Stony Brook, Stony Brook, New York 11794-5215[2]; and Departamento de Microbiología II, Universidad Complutense de Madrid, CP 28040 Madrid, Spain[3]

Received 9 October 2006/Accepted 15 December 2006

The *GAS* multigene family of *Saccharomyces cerevisiae* is composed of five paralogs (*GAS1* to *GAS5*). *GAS1* is the only one of these genes that has been characterized to date. It encodes a glycosylphosphatidylinositol-anchored protein functioning as a β(1,3)-glucan elongase and required for proper cell wall assembly during vegetative growth. In this study, we characterize the roles of the *GAS2* and *GAS4* genes. These genes are expressed exclusively during sporulation. Their mRNA levels showed a peak at 7 h from induction of sporulation and then decreased. Gas2 and Gas4 proteins were detected and reached maximum levels between 8 and 10 h from induction of sporulation, a time roughly coincident with spore wall assembly. The double null *gas2 gas4* diploid mutant showed a severe reduction in the efficiency of sporulation, an increased permeability of the spores to exogenous substances, and production of inviable spores, whereas the single *gas2* and *gas4* null diploids were similar to the parental strain. An analysis of spore ultrastructure indicated that the loss of Gas2 and Gas4 proteins affected the proper attachment of the glucan to the chitosan layer, probably as a consequence of the lack of coherence of the glucan layer. The ectopic expression of *GAS2* and *GAS4* genes in a *gas1* null mutant revealed that these proteins are redundant versions of Gas1p specialized to function in a compartment at a pH value close to neutral.

During vegetative growth, *Saccharomyces cerevisiae* yeast cells produce and secrete cell wall components that are incorporated into the expanding extracellular matrix through a cross-linking process. The resulting matrix gives enough resistance to the cell to counteract a higher internal pressure and provides a barrier against external agents. For this crucial role in maintaining cell integrity, the cell wall is essential for the viability of yeast and fungal cells. Several enzymes cooperate in the biogenesis of the cell wall during vegetative growth (13, 21, 27). At the level of the plasma membrane, a β(1,3)-glucan synthase complex that has Fks1p as a catalytic component synthesizes and extrudes β(1,3)-glucan, the most abundant polysaccharide, representing about 40 to 50% of cell wall dry weight (11). Chitin synthases CSI, CSII, and CSIII, whose catalytic subunits are Chs1p, Chs2p, and Chs3p, respectively, catalyze the synthesis of chitin that constitutes about 1 to 2% of cell wall dry weight. Mannoproteins (~40% of cell wall dry weight) are produced and processed along the secretory pathway, while it is still controversial whether β(1,6)-glucan (~10 to 20% of cell wall dry weight) is produced at the level of the plasma membrane or along the secretory pathway (27, 28, 31, 41). The polymers are cross-linked outside the plasma membrane boundary, and a β(1,3)-glucan fibrillar network, to which β(1,6)-glucan and chitin chains are linked, is formed (22, 23, 27). Mannoproteins can be cross-linked to the β(1,3)-glucan network either indirectly, through a remnant of a glycosylphosphatidylinositol (GPI) bound to a β(1,6)-glucan chain, or directly, through an alkaline-sensitive linkage that recently was shown to involve glutamine residues (10, 12, 19, 23, 45). It has been determined by electron microscopy analysis that the typical vegetative cell wall is organized with the inner layers constituted of glucan and chitin and the outer layer formed by a brush-like mannoprotein shell that can be removed by the action of proteases (46). Additionally, chitin is deposited at the bud neck and in the primary septum and only a tiny amount is located in the lateral cell walls. This organized structure of cross-linked macromolecules results from the coordinated actions of several extracellular enzymes, most of which have still to be characterized, and from the integration of these extracellular assembly processes with the cytoskeleton and polarity machinery of the cell (13).

The cell wall changes in composition and architecture during the yeast growth cycle and the life cycle and in response to stress (2, 13, 14, 21, 25). Diploid cells placed in the presence of a nonfermentable carbon source, such as acetate or glycerol, in the absence of glucose and of a nitrogen source, undergo the process of meiosis and sporulation that leads to the formation of four haploid nuclei encapsulated in four ascospores. The anucleate mother cell is transformed into an ascus (reviewed in reference 33). Ascospore cell wall assembly begins after the closure of the prospore membrane that engulfs a haploid nucleus (33). Two remarkable features of this process are that (i) the spore wall is formed in the lumen between the two mem-

* Corresponding author. Mailing address: Dipartimento di Scienze Biomolecolari e Biotecnologie, Università degli Studi di Milano, Via Celoria 26, 20133 Milano, Italy. Phone: 39-(0)2-5031 4919. Fax: 39-(0)2-5031 4912. E-mail: Laura.Popolo@unimi.it.

† Present address: DIBIT, San Raffaele Scientific Institute, Via Olgettina 58, 20132 Milano, Italy.

▽ Published ahead of print on 22 December 2006.

branes derived from the closure of the prospore membrane and therefore is created in the absence of a preexisting structure and (ii) the layered organization of the spore wall follows a sequential program that differs from that occurring in vegetative growth. Moreover, the spore wall contains unique constituents, such as dityrosine and chitosan (8, 33). For these reasons, spore wall assembly is an interesting model of de novo formation of a supramolecular biological structure (33). Outside the plasma membrane of the spore, the two inner layers of the spore wall are made of mannoproteins and glucan that occur in an inverse orientation with respect to the vegetative cell wall (24). The external layers are formed by chitosan, a deacetylated form of chitin, and dityrosine, an insoluble arrangement of D- and L-tyrosine residues that confers the high resistance to external stresses that is typical of spores. The ascospores are interconnected by chitosan-containing structures that form the interspore bridges (9).

Meiosis and sporulation involve the induction of many genes that have been divided into categories based on their temporal expression profiles (7, 38). Many genes involved in spore wall formation and maturation are classified as middle, middle-late, and late genes (7, 33, 38). Some of these genes are specific for sporulation and have no counterparts. Examples of such genes are *CDA1* and *CDA2*, encoding two isoforms of chitin-deacetylase, and *DIT1* and *DIT2*, encoding the first enzymes in the synthesis pathway of dityrosine. Others are paralogs of genes that function in vegetative growth, such as *SHC1*, which replaces *CHS4* in regulating Chs3p during sporulation, and *CRR1*, which encodes a sporulation-specific putative transglycosidase and is related to the *CRH1* and *CRH2* genes that are expressed only during vegetative growth (16, 40). Thus, the peculiar architecture and composition of the spore wall require the action of gene products that have to be produced specifically during this developmental process.

The *GAS* multigene family is composed of five paralogs, from *GAS1* to *GAS5* (37). *GAS1* is the best characterized of these genes. It encodes a GPI-anchored glycoprotein localized predominantly in the plasma membrane and recently shown to also be covalently bound to the cell wall (37, 45). It is a key enzyme in yeast cell wall assembly that, through its β(1,3)-glucanosyltransferase activity, cleaves and religates β(1,3)-glucans, elongating the linear chains (6, 32). *GAS1* is expressed during vegetative growth, and its inactivation causes a decrease in the amount of cell wall β(1,3)-glucans that is compensated for by several changes in the cell wall composition, the most remarkable of which is an increase in chitin and mannoproteins (35, 39). This defect in cell wall assembly leads to a round-cell morphology, failure in cell separation, reduced growth rate, and resistance to Zymolyase that are phenotypic traits typical of the mutant (35, 36).

The roles of the other *GAS* genes have not yet been investigated. In this work, we describe the characterization of the *GAS2-GAS4* gene pair. We analyzed their expression profile, monitored the Gas2 and Gas4 protein levels during sporulation, and determined that together they are essential for proper spore wall assembly. Moreover, we found that Gas2p and Gas4p can replace Gas1p in vegetative growth, but only in media at near-neutral pH values.

MATERIALS AND METHODS

Yeast strains and growth conditions. The strains used were derived from the sporulation-proficient strains W303 and SK1 and are listed in Table 1. Cells were grown in batches at 30°C in synthetic dextrose (SD) minimal medium (Difco yeast nitrogen base without amino acids at 6.7 g/liter, 2% glucose), to which the required supplements were added at concentrations of 50 mg/liter for the amino acids and uracil and 100 mg/liter for adenine, or in YPD (1% yeast extract, 2% Bacto peptone, 2% glucose). For buffered medium, 10 g/liter MES [2-(*N*-morpholino)ethanesulfonic acid] was added and the pH was brought to 6.5 or 5.5. For solid media, 2% agar was added to YPD or SD medium (YPDA and SDA, respectively). Growth was monitored as the increase in absorbance at 450 nm (A_{450}). Duplication time (T_d) was calculated by the equation $T_d = \ln 2/k$, where k, the growth rate constant, is the slope of the line obtained by linear regression on a semilogarithmic plot of the A_{450} values, whereas the growth rate, μ (h^{-1}), was calculated as $1/T_d$.

For tetrad dissection, diploids were sporulated on solid plates of new sporulation medium (NSM; 8.2 g sodium acetate, 1.9 g KCl, 0.35 g $MgSO_4$, 1.2 g NaCl, 15 g agar per liter) at 24°C. Spore germination was carried out at 30°C on YPDA. Sporulation in liquid media was carried out as follows: cells were grown in YPD, and during exponential growth phase, they were collected by centrifugation, washed once with YPA (1% yeast extract, 2% Bacto peptone, and 2% potassium acetate) and inoculated into YPA at an initial optical density of 450 nm (OD_{450}) of 0.2. Cells were grown overnight, and the following morning, they were collected and washed with sporulation medium (SPM-1; 1% potassium acetate for SK1, supplemented with 20 mg/liter adenine for diploid W303 [W303^2]) before being inoculated in prewarmed SPM-1 at a concentration of about 10^7 cells/ml (OD_{450} of about 1 to 1.5). In order to obtain a high efficiency of sporulation, the ratio of the volume of the culture to the volume of the flask was 1:10. Cultures were allowed to sporulate under vigorous shaking for 24 to 48 h at 30°C. Diploid strains harboring YEp24-derived plasmids were inoculated into liquid, semidefined presporulation medium (SA; 10 g potassium acetate, 6.7 g yeast nitrogen base without amino acids, 1 g yeast extract in 1 liter of 0.05 phthalate buffer [pH 5] [42]) and grown for 3 to 4 generations. Cells were sporulated in SPM-2, a 0.3% potassium acetate solution (17).

Quantification of mRNA using real-time quantitative reverse transcriptase PCR (RT-PCR). Total RNA was extracted from cells (5×10^7) collected at different time intervals after transfer to sporulation medium, using an RNeasy mini kit combined with the RNase-free DNase on-column treatment (QIAGEN GmbH, Hilden, Germany). First-strand cDNAs were synthesized from 1.8 μg of total RNA using a reverse transcription system (Promega) following the recommendations of the manufacturer, except that the incubation time of the reverse transcription reaction was extended to 45 min. As a control for genomic contamination, the same reactions were performed in the absence or presence of reverse transcriptase. Real-time PCR was performed using an ABI 7700 instrument (Applied Biosystems) in a final volume of 20 μl containing 5 μl of a 100-fold dilution of the reverse transcription reaction and 12.5 μl of 2× SYBR green PCR master mix (Applied Biosystems) together with the specific forward and reverse *GAS2*, *GAS4*, or *ACT1* primers (Table 2). The primers were designed using Primer Express software 2.0 (Applied Biosystems). Each primer couple was complementary to portions that are specific for each *GAS* open reading frame (ORF). The real-time PCR conditions were selected according to the universal conditions (default) recommended by the manufacturer of the instrument. Each cDNA was assayed in at least duplicate PCRs for two independent experiments. Basic analysis was performed using SDS 1.9.1 software (Applied Biosystems). For further elaboration of the data, the Livak method (30) was used. Briefly, from each duplicate reaction, a ΔC_T was calculated by subtracting the average C_T value of *ACT1* from the average C_T value of the gene of interest for the same time. Then the difference between the ΔC_T at any time and the ΔC_T at time zero was calculated ($\Delta\Delta C_T$). The plotted values are $2^{-\Delta\Delta C_T}$.

Cloning of *GAS2* and *GAS4* genes from SK1. *GAS2* (YLR343W) and *GAS4* (YOL132W) genes, spanning 400 bp upstream and 300 bp downstream from the coding region, were amplified by PCR from genomic DNA with the following pairs of primers containing restriction sites: *Nhe*-GAS2 and GAS2-*Sal*down and *Nhe*-GAS4 and *Sal*-GAS4 (Table 2). The amplified *GAS2* and *GAS4* products were cloned in TA-TOPO cloning vector (Invitrogen) and generated the pER-2 and pER-4 plasmids. Sequence verification was carried out by sequencing both strands of DNA plasmids extracted from at least three different clones. Single-nucleotide polymorphisms were found, in agreement with the reported polymorphism of the SK1 strain compared to S288c (38). In the *GAS2* 5′-flanking region, a C-to-T transition and an A-to-T transversion were found at nucleotides −57 and −26 from the initiation codon (the A of ATG was set as nucleotide 1). In the *GAS2* open reading frame, the C-to-T and A-to-G transitions, the T-to-A trans-

TABLE 1. *S. cerevisiae* strains used

Strain	Genotype	Source
SK1 background		
AN117-4B	*MAT*α *arg4 his3 ho*::*LYS2 leu2 lys2 rme1*::*LEU2 trp1 ura3*	A. Neiman
AN117-16D	*MAT***a** *his3 ho*::*LYS2 leu2 lys2 trp1 ura3*	A. Neiman
AN120	*MAT***a**/*MAT*α *arg4*/*ARG4 his3*/*his3 ho*::*LYS2*/*ho*::*LYS2 leu2*/*leu2 lys2*/*lys2 rme1*::*LEU2*/*RME1 trp1*/*trp1 ura3*/*ura3* (cross of AN117-4B and AN117-16D)	A. Neiman
ER300	AN117-4B *gas2*::*HIS3*	This study
ER303	*MAT***a**/M*AT*α *arg4*/*ARG4 gas2*::*HIS3*/*GAS2 his3*/*his3 ho*::*LYS2*/*ho*::*LYS2 leu2*/*leu2 lys2*/*lys2 rme1*::*LEU2*/*RME1 trp1*/*trp1 ura3*/*ura3* (cross of ER300 and AN117-16D)	This study
ER303-6A	*MAT***a** *gas2*::*HIS3 his3 ho*::*LYS2 leu2 lys2 trp1 ura3* (segregant from ER303)	This study
ER301	AN117-4B *gas4*::*KanMX2*	This study
ER304	*MAT***a**/M*AT*α *arg4*/*ARG4 gas4*::*KanMX2*/*GAS4 his3*/*his3 ho*::*LYS2*/*ho*::*LYS2 leu2*/*leu2 lys2*/*lys2 rme1*::*LEU2*/*RME1 trp1*/*trp1 ura3*/*ura3* (cross of ER301 and AN117-16D)	This study
ER304-3B	*MAT***a** *gas4*::*KanMX2 his3 ho*::*LYS2 leu2 lys2 trp1 ura3* (segregant from ER304)	This study
ER308	*MAT***a**/M*AT*α *arg4*/*ARG4 gas2*::*HIS3*/*GAS2 gas4*::*KanMX*/*GAS4 his3*/*his3 ho*::*LYS2*/*ho*::*LYS2 leu2*/*leu lys2*/*lys rme1*::*LEU2*/*RME1 trp1*/*trp1 ura3*/*ura3* (cross of ER300 and ER304-3B)	This study
ER308-9C	*MAT*α *arg4 gas2*::*HIS3 gas4*::*LEU2 his3 ho*::*LYS2 leu2 lys2 rme1*::*LEU2 trp1 ura3* (segregant from ER308)	This study
ER308-13A	*MAT***a** *gas2*::*HIS3 gas4*::*LEU2 his3 ho*::*LYS2 leu2 lys2 ura3 trp1* (segregant from ER308)	This study
ER306	*MAT***a**/*MAT*α *arg4*/*ARG4 gas2*::*HIS3*/*gas2*::*HIS3 his3*/*his3 ho*::*LYS2*/*ho*::*LYS2 leu2*/*leu2 lys2*/*lys2 rme1*::*LEU2*/*RME1 trp1*/*trp1 ura3*/*ura3* (cross of ER303-6A and ER300)	This study
ER307	*MAT***a**/*MAT*α *arg4*/*ARG4 gas4*::*KanMX2*/*gas4*::*KanMX2 his3*/*his3 ho*::*LYS2*/*ho*::*LYS2 leu2*/*leu2 lys2*/*lys2 rme1*::*LEU2*/*RME1 trp1*/*trp1 ura3*/*ura3* (cross of ER304-3B and ER301)	This study
ER309	*MAT***a**/*MAT*α *arg4*/*ARG4 gas2*::*HIS3*/*gas2*::*HIS3 gas4*::*KanMX2*/*gas4*::*KanMX2 his3*/*his3 ho*::*LYS2*/*ho*::*LYS2 leu2*/*leu2 lys2*/*lys2 rme1*::*LEU2*/*RME1 trp1*/*trp1 ura3*/*ura3* (cross of ER308-13A and ER308-9C)	This study
ER310	AN120[2 μm-*URA3*(YEp24)]	This study
ER311	AN120[2 μm-*GAS2*–*URA3*(pYER-2)]	This study
ER312	ER306[2 μm-*GAS2*–*URA3*(pYER-2)]	This study
ER313	ER309[2 μm-*GAS2*–*URA3*(pYER-2)]	This study
ER314	ER306[2 μm-*GAS2*-3xHA–*URA3*(pYER-2-HA)]	This study
ER315	ER309[2 μm-*GAS2*-3xHA–*URA3*(pYER-2-HA)]	This study
ER316	AN120[2 μm-*GAS4*–*URA3*(YER-4)]	This study
ER317	ER309[2 μm-*URA3*(YEp24)]	This study
W303 background		
W303-1A	*MAT***a** *ade2-1 can1-100 his3-11,15 leu2-3,112 trp1-1 ura3-1*	P. P. Slominski
W303-1B	*MAT*α *ade2-1 can1-100 his3-11,15 leu2-3,112 trp1-1 ura3-1*	P. P. Slominski
WB2d	*gas1*::*LEU2* (derived from W303-1B)	Vai et al. (1991)
G2HB	W303-1B *gas2*::*HIS3*	This study
G4LB	W303-1B *gas4*::*KanMX2*	This study
Y0	Wb2d[2 μm-*URA3*(pY0)]	This study
Y1	WB2d[2 μm-*URA3*–*GAS1*(pY1)]	This study
Y2	WB2d[2 μm-*URA3*–P_{GAS1}-*GAS2* ORF(pY2)]	This study
Y4	WB2d[2 μm-*URA3*–P_{GAS1}-*GAS4* ORF(pY4)]	This study
W303^{2a}	*MAT***a**/*MAT*α *ade2-1*/*ade2-1 can1-100*/*can1-100 his3-11,15*/*his3-11,15 leu2-3,112*/*leu2-3,112 trp1-1*/*trp1-1 ura3-1*/*ura3-1* (cross of W303-1A and W303-1B)	This study
G2D^2	*MAT***a**/*MAT*α *ade2-1*/*ade2-1 can1-100*/*can1-100 gas2*::*HIS3*/*gas2*::*HIS3 his3-11,15*/*his3-11,15 leu2-3,112*/*leu2-3,112 trp1-1*/*trp1-1 ura3-1*/*ura3-1*	This study
G4D^2	*MAT***a**/*MAT*α *ade2-1*/*ade2-1 can1-100*/*can1-100 gas4*::*LEU2*/*gas4*::*LEU2 his3-11,15*/*his3-11,15 leu2-3,112*/*leu2-3,112 trp1-1*/*trp1-1 ura3-1*/*ura3-1*	This study
G24D^2	*MAT***a**/*MAT*α *ade2-1*/*ade2-1 can1-100*/*can1-100 gas2*::*HIS3*/*gas2*::*HIS3 gas4*::*LEU2*/*gas4*::*LEU2 his3-11,15*/*his3-11,15 leu2-3,112*/*leu2-3,112 trp1-1*/*trp1-1 ura3-1*/*ura3-1*	This study

[a] A superscript 2 indicates a diploid.

version, and two G-to-A transitions were found at nucleotides 656, 1138, 1283, 1370, and 1644, respectively, causing the following amino acid substitutions: A219 to V, K380 to E, L428 to H, C457 to Y, and M548 to I. In the 3′-flanking region, a C-to-A transversion was present. In the *GAS4* 5′-flanking region, the following point mutations were found: T to C, G to A, T to C, and A to T, at nucleotides −302, −297, −262, and −257, respectively, and the insertion of an A between nucleotides −28 and −29. In the *GAS4* open reading frame, an A-to-T and a T-to-C base substitution were found at nucleotides 66 and 1023, respectively, but these changes were silent. Yeast plasmids pYER-2 and pYER-4 were obtained by cloning the NheI/SalI fragment from pER-2 and pER-4 into the corresponding sites of the YEp24 vector.

Construction of the *GAS2*-3xHA fusion. The fusion gene was obtained by overlap extension PCR (18). In the first PCR step, two overlapping fragments of the designed *GAS2*-3xHA fusion were amplified using two sets of primers: forward primer *Nhe*-GAS2 and reverse primer HA3-Rev and GAS2-*Sal*down with forward primer HA3-for (Table 2). In these primers, the overlapping segments of the sequence encoding the 3 × hemagglutinin (HA) epitopes were incorporated. The complete 3 × HA sequence, encoding 30 amino acids (YPY DVPDYAGYPYDVPDYAGSYPYDVPDYA; MW:3471.65), was obtained by overlap between the amplified fragments. Pairing of equimolar quantities of gel-purified PCR products was used to direct a preextension PCR consisting of 15 cycles performed without primers as described in reference 1. A second PCR step of 15 cycles in the presence of primers *Nhe*-GAS2 and GAS2-*Sal*down was performed. The amplified fragment of about 2.5 kbp was cloned in TA-TOPO cloning vector and introduced into *Escherichia coli* TOP10 cells. The DNA plasmids were scored for the presence of BamHI, a diagnostic site for the

TABLE 2. Oligonucleotide sequences used

Use and name	Sequence (5′ to 3′)
Quantitative RT-PCR	
GAS2 Forward	CATCGCGTAGCAAGGAAAGTT
GAS2 Reverse	ATGCGATGGTGCCGTCA
GAS4 Forward	AAACACCGGAATTCTGCCTCTA
GAS4 Reverse	AAAGCAAACACAACCCAAGAGG
ACT1 Forward	ACGAAAGATTCAGAGCCCCA
ACT1 Reverse	GCAGATTCCAAACCCAAAACA
Cloning *GAS2* and *GAS4*[a]	
Nhe-GAS2	AGCATATTCGACTGAGCTAGCACTCTC AAGATGTTGCAAATACGG
GAS2-*Sal*down	ATCGTCGGGCTCAGTCGACCAATTAAA ACGTTACGAACTGTCA
Nhe-GAS4	AGCATATTCGACTGAGCTAGCGACAG AACACCCTCATCC
Sal-GAS4	ATCGTCGGGCTCAGTCGACAATGGACT CGTACTGTG
Internal tagging of *GAS2*[b]	
HA3-Rev	**TGCATAGTCCGGGACGTCATACGGATAGC CCGCATAGTCAGGAACATCGTATGGGT** ATGATTTTGAATAATCGCC
HA3-for	**CCGTATGACGTCCCGGACTATGCAGGATC CTATCCATATGACGTTCCAGATTACGCT** AATCCATCGCGTAGCAAG
Inactivation of *GAS2* and *GAS4*[c]	
Gas2Hfor	AACTCGAGGTACTTGAAACTTTTCAGT TAAGTATGAACAAGA**CCAGCTGAAGC TTCGTAC**
Gas2Hrev	TTCCAGCAGCTATCATAGAAATTAGAA GTATAACAAACCCTG**GATGAATTCGA GCTCGTT**
Gas4Lfor	TCGAGCACCTTTATTTTTCTAATTTTGG AGTTAGTTGTACTGTGTGAAGCTTCA GTCCAC**CTCGAGGAGAACTTCTAG**
Gas4Lrev	AAAAGCAAACACAACCCAAGAGGTAA CAATGGGCCGGAAATAGAGGCAGA ATTCCGGTGT**GTCGACTACGTCGT TAAG**
Gas4Kfor	TCGAGCACCTTTATTTTTCTAATTTTGG AGTTAGTTGTACTGTGTGAAGCTTCA GTCCAC**GATATCAAGCTTGCCTCG**
Gas4Krev	AAAAGCAAACACAACCCAAGAGGTAA CAATGGGCCGGAAATAGAGGCAGA ATTCCGGTGT**GTCGACACTGGATG GCGG**
Gas2Test	TCGGTGTCAGTAATTCTG
Gas2Valle	ACTGCCTGTACTGCTCAT
Gas2orf	CCACACCATTCGTACATA
Gas2orfrev	TATGTACGAATGGTGTGG
HIS3orfup	**TGCATGTTACCTGCTTAT**
HIS3orfdown	**ATAAGCAGGTAACATGCA**
Gas4Test	GTATTGTAAGGTGAGACT
Gas4Valle	GGACTCGTACTGTGCATA
Gas4orf	ATTCTCTGGCTTATCATC
Gas4orfrev	GATGATAAGCCAGAGAAT
Leu	**GACACCATCACCATCGTC**
Leurev	**GACGATGGTGATGGTGTC**
KanMX2	**CAACAGGCCAGCCATTAC**
KanMX2Rev	**GTAATGGCTGGCCTGTTG**

[a] The NheI and SalI restriction sites are underlined.

[b] The coding sequences for 3 × HA are in boldface, and the overlapping segments are underlined.

[c] Sequences internal to the *KANMX2* and *HIS3MX6* cassettes and the *LEU2* marker are in boldface.

presence of the 3 × HA sequence. The positive plasmids were sequenced and named pER-2-HA. The NheI/SalI fragment from the plasmid with the correct sequence was cloned into the corresponding site of the pYEp24 vector, generating pYER-2-HA.

Construction of mutant strains. The oligonucleotides used to construct the null mutations and to test them are listed in Table 2. The short-homology PCR technique, followed by one-step gene disruption, was used for the construction of the mutant strains. Plasmid pFA6a-HIS3MX6, containing the module HIS3MX6 with the *his5*$^+$ gene from *Schizosaccharomyces pombe*, was used to amplify a PCR fragment used to inactivate *GAS2*. The 1.4-kbp PCR fragment, carrying 42 nucleotides at the ends complementary to the −32-to-10 and 1616-to-1657 segments from the start codon of *GAS2*, was used to transform both of the haploid strains W303-1B and AN117-4B, giving rise to strains G2HB and ER300, respectively (Table 1). pFA6a-KanMX2, which contains the *KANMX2* module, was used to amplify a 1.5-kbp PCR fragment used to inactivate *GAS4* in the AN117-4B strain. The PCR fragment carried sequences complementary to the 13-to-72 and 1332-to-1391 regions from ATG of *GAS4* at the ends. To inactivate *GAS4* in the W303-1B strain, pBSG7L13 containing the *LEU2* marker cassette was used as the template. A PCR fragment of about 2.3 kbp, carrying sequences complementary to nucleotides 13 to 72 and 1332 to 13391 from the *GAS4* ATG at the ends, was amplified with oligonucleotides GAS4Lfor and GAS4Lrev and used to transform the W303-1B strain, creating strain G4LB (Table 1). *S. cerevisiae* cells were transformed with an S.C. EasyComp transformation kit (Invitrogen). About 50 ng of genomic DNA isolated from the transformant clones was subjected to three diagnostic PCR tests to verify correct integration (the primers used are listed in Table 2). The W303-derived haploid *gas2*Δ and *gas4*Δ null mutants were obtained and crossed with the strain of opposite mating type (W303-1A). The diploids were obtained from zygotes by micromanipulation of conjugating meiotic segregants carrying the desired mutations. In the SK1 genetic background, the haploid AN117-4B strain carrying the *gas2*Δ (ER300) or the *gas4*Δ (ER301) mutation was crossed with the AN117-16D strain. The resulting heterozygous strains (ER303 and ER304) were selected by marker complementation and induced to sporulate. Meiotic segregants carrying the *gas2* or *gas4* null mutation together with the genetic markers required for diploid selection were backcrossed with ER300 or ER301 to generate *gas2*Δ/*gas2*Δ (ER306), *gas4*Δ/*gas4*Δ (ER307), and *gas2*Δ/*gas2*Δ *gas4*Δ/*gas4*Δ (ER309) null diploids.

Plasmid construction for testing the complementation of the *gas1* phenotype. The coding sequences of *GAS2* and *GAS4* genes, previously cloned from W303-1B genomic DNA, were placed under the control of the *GAS1* promoter (P_{GAS1}) in the high-copy YEp24 vector. The plasmids were a kind gift of M. Vai (Università di Milano-Bicocca). Briefly, a 4-kbp NcoI/BamHI fragment containing the *GAS1* 5′-flanking region and the *GAS2* ORF and its downstream sequence was excised from plasmid pG2 derived from pGEM7Zf(+) and cloned into the corresponding sites in YEp24. A 3.8-kbp NcoI-BamHI fragment containing the *GAS4* ORF and termination sequences cloned downstream from the *GAS1* upstream region was excised from plasmid pG4 and inserted in YEp24. YEp24, YEp24-[P_{GAS1}-*GAS2*], and YEp24-[P_{GAS1}-*GAS4*] were used to transform *gas1*Δ cells (WB2d) to yield strains Y0, Y2, and Y4. The strain harboring YEp24 containing the *GAS1* gene and its flanking regions was described previously (43) and is named Y1 in this work.

Light microscopy. Cells were routinely observed by phase-contrast microscopy, and sporulation was scored by counting at least 200 cells after a mild sonication.

DNA staining. Cells were collected by centrifugation at 13,000 rpm for 1 min, and the pellet was washed twice with distilled water (dH_2O). Then cells were fixed with ethanol and preserved at 4°C until use. At the time of the analysis, cells were washed with dH_2O and pellets were resuspended in a solution of 0.125 μg/ml of DAPI (4,6-diamidine-phenylindole). After a 10-min incubation in the dark, cells were washed twice with dH_2O and examined in the fluorescence microscope. Cells with 1, 2, or 4 nuclei were counted.

Microscopic observation of dityrosine. The observation of the natural fluorescence of dityrosine was performed essentially as described previously (4). Sporulating cells were collected by centrifugation and resuspended in 1 ml of 5% aqueous ammonia. Cells were observed under the fluorescent microscope using UV light (DAPI filter).

Assay for the presence of dityrosine. An assay for the presence of dityrosine was performed as described previously (3, 26). Cells were streaked onto solid YPD. After a 2-day incubation at 30°C, the patches were then replica plated onto nitrocellulose filters that had been placed on YPD plates. After a 1-day incubation at 30°C, the filters were transferred to solid sporulation medium (SPM-1), colony-side up, and placed at 30°C for 3 days. To remove the ascal walls, the filters were placed in a 9-cm petri dish containing 400 μl of water, 140 μl of glusulase (from *Helix pomatia*; Roche), and 30 μl of 2-mercaptoethanol. After 5 h at 30°C, the filters were transferred to a dish containing 500 μl of 30% aqueous ammonia. The filters were photographed under UV light (312 nm) using a digital camera.

Permeability and Zymolyase assays. For testing permeability to calcofluor, an aliquot corresponding to 10^7 cells was withdrawn from the culture and mildly sonicated. Cells were pelleted, washed with 500 μl of dH_2O, and resuspended in 500 μl of a solution of 10 μg/ml of calcofluor white (CW; Sigma). After a 1-min incubation at room temperature, cells were centrifuged and washed three times with 800 μl of dH_2O. Cells were examined with an Olympus BX60 microscope connected to a DC290 Kodak digital camera. Zymolyase sensitivity was quantitated essentially as described previously (8): 100 μl of sporulated culture (approximately 0.2 at OD_{450}) was washed and resuspended in 1,090 μl of dH_2O. Ten microliters of Zymolyase 100T (ICN Biomedicals, Aurora, OH) at 10 mg/ml was added, and the cells were incubated at 37°C. At 10-min intervals, 100 μl of cells was withdrawn, diluted in dH_2O, and plated to determine the titer of viable cells.

Test of sensitivity of growth to calcolfuor. Five microliters from a concentrated suspension of cells (total, 8 at OD_{450}) and 5 μl from 1:10 serial dilutions of the concentrated suspension were spotted on SDA or buffered SDA plates in the absence or presence of 2, 5, 10, 25, or 50 μg of CW per ml. Growth was checked after 2 days at 30°C.

Electron microscopy. Cells were prepared for analysis on the transmission electron microscope (TEM) using osmium tetroxide and sodium thiocarbohydrazide staining as described previously (8). Images were collected on an FEI BioTwin microscope at 80 kV using an AMT digital camera (Advanced Microscopy Techniques Corp., Danvers, MA). For scanning electron microscopy (SEM) studies, spheroplasts were sporulated and prepared as described previously (8), except that spores were released from the ascal membrane by washes in 0.1% sodium dodecyl sulfate (SDS). Images were collected on a LEO1550 SEM at 2.5 kV using an in-lens detector.

Extract preparation, electrophoresis, and immunoblotting. Sporulating cells (2×10^8) were collected by filtration, washed, and resuspended in ice-cold dH_2O. After a 2-min centrifugation at 4°C, the pellets were frozen quickly and stored at −20°C. After thawing, 500 μl of SB-minus buffer (0.0625 M Tris-HCl [pH 6.8], 5% SDS) supplemented with protease inhibitors (1 mM phenylmethylsulfonyl fluoride and a complete protease inhibitor cocktail [Roche] prepared as a 25× stock in dH_2O) was added to each pellet. After the addition of an equal volume of cold glass beads, cells were broken by shaking in a bead miller four times for 1 min alternating with 1-min incubations on ice. Next, unbroken cells and glass beads were removed by a 5-min centrifugation at 13,000 rpm at 4°C. For determination of the protein concentration by the DC protein assay (Bio-Rad), aliquots of 10 to 20 μl of the cleared lysates were used in duplicate for each sample. For the SDS-polyacrylamide gel electrophoresis (PAGE) analysis, appropriate amounts of a concentrated solution were added to the lysate in order to bring the sample to a final concentration of 10% glycerol, 5% β-mercaptoethanol, and 0.02% bromophenol blue. Before loading, samples were denatured at 100°C for 3 min. Slab gels of 8% polyacryamide gels were used for extract separation. Immunoblotting was carried out as previously described (15). A monoclonal antibody, HA.11 (clone 16B12), from Covance (Berkeley, CA) was used to recognize the HA epitope and diluted 1:6,000 in Tris-buffered saline–bovine serum albumin, 0.3% Tween 20. Monoclonal mouse anti-actin antibody, clone C4 (MP Biomedicals), was used at a dilution of 1:1,000. Anti-Gas4p serum was obtained by immunizing rabbits with a soluble six-His-tagged form of Gas4p produced in *Pichia pastoris* (unpublished data). The immunization procedure was carried out by Areta International S.r.l. (Gerenzano, Varese, Italy). The optimal dilution of anti-Gas4p serum was 1:1,000 in Tris-buffered saline–bovine serum albumin, 0.2% Tween-20. Peroxidase-conjugated affinity-purified $F(ab')_2$ fragment donkey anti-rabbit or anti-mouse immunoglobulin G was from Jackson Laboratories and used at a dilution of 1:10,000. Bound antibodies were revealed using ECL Western blotting detection reagents (Amersham Pharmacia Biotech). Densitometric measurements of undersaturated films were performed using the Scion Image program.

EndoH treatment. Sporulating cells (2×10^8) were collected by filtration, frozen quickly, and stored at −20°C. After thawing, 400 μl of deglycosylation buffer (300 mM sodium citrate buffer [pH 5.5], 0.4% SDS, 2% β-mercaptoethanol) supplemented with protease inhibitors was added and cells were broken as described above. Then, samples were denatured at 100°C for 3 min, and unbroken cells and glass beads were removed by a 2-min centrifugation at 13,000 rpm. The cleared lysate was added with an equal volume of 300 mM sodium citrate buffer, pH 5.5, supplemented with protease inhibitors, in order to bring the samples to a final concentration of 0.2% SDS and 1% β-mercaptoethanol. Aliquots of 45 μl were supplied with 100 mU of endo-β-acetylglucosaminidase H (EndoH) (Roche) or with an equal volume of sodium citrate buffer. After a 4-h or 16-h incubation at 37°C, samples were prepared for electrophoresis as described above.

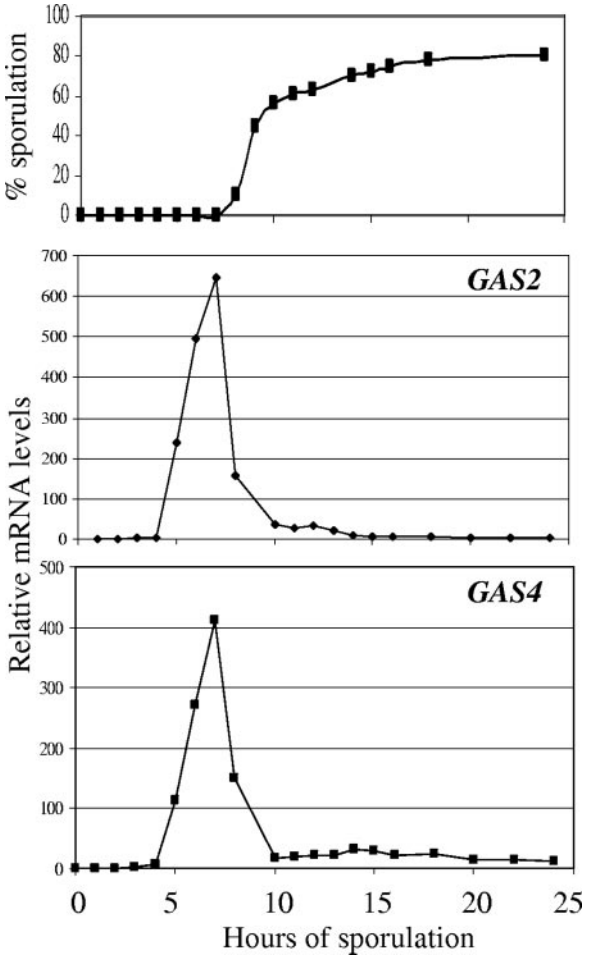

FIG. 1. Time course of *GAS2* and *GAS4* transcription during sporulation. Upper panel, kinetics of sporulation of the SK1 strain after shifting from YPA to SPM-1. Central and lower panels, levels of mRNA for *GAS2* and *GAS4* were measured by real-time quantitative RT-PCR. Relative mRNA levels are indicated with respect to zero time and were calculated as described in Materials and Methods.

RESULTS

Expression profiles of *GAS2* and *GAS4* genes during meiosis and sporulation. The levels of *GAS2* and *GAS4* mRNA were determined in a sporulation time course. An SK1 background strain was used, since it sporulates with a high degree of synchrony, completing the process in 24 h, as shown in Fig. 1, upper panel. At different time intervals from the induction of sporulation, total RNA was extracted from SK1 cells and used for a quantitative real-time RT-PCR analysis. Actin mRNA was chosen as a reference transcript, since the expression of the actin gene (*ACT1*) does not fluctuate significantly in sporulating SK1 cells (38). As shown in Fig. 1, central and lower panels, the expression of both *GAS2* and *GAS4* was limited to a short time span. A peak of expression occurred at 7 h from induction of sporulation, and by 10 h, the mRNA levels were greatly decreased. The comparison of the cycle threshold values for *GAS2* (C_T = 21.08) and *GAS4* (C_T = 18.74), obtained at 7 h in the same amplification experiment, indicated that *GAS4* is expressed at a higher level than *GAS2*. Moreover,

TABLE 3. Effects on sporulation of deletions, of overexpression of *GAS2* and *GAS4* genes, and of *GAS2* tagging

Function and strain	Genotype	Distribution of ascal types (%)[a]				
		Unsporulated	Monad	Dyad	Triad	Tetrad
Deletion mutants[b]						
AN120	*GAS2*/*GAS2 GAS4*/*GAS4*	20.6 ± 5.5	0	4.8 ± 3.5	0.5 ± 0.3	68.1 ± 3.7
ER306	*gas2*Δ/*gas2*Δ	21 ± 6.5	0.6 ± 0.2	6 ± 0.5	7.2 ± 0.3	65.2 ± 6.2
ER307	*gas4*Δ/*gas4*Δ	24.3 ± 1.2	0	3.8 ± 1.5	1.5 ± 0.5	70.5 ± 2.8
ER309	*gas2*Δ *gas4*Δ/*gas2*Δ *gas4*Δ	67.4 ± 11.6[d]	14.3 ± 8.2	13 ± 5.3	4.6 ± 3.2	0.7 ± 0.6
Overexpressed genes[c]						
ER310	*GAS2*/*GAS2 GAS4*/*GAS4*[2 μm-*URA3*]	8.1 ± 3.4	0.4 ± 0.2	8.5 ± 2.9	11.4 ± 3.8	71.6 ± 3.2
ER311	*GAS2*/*GAS2 GAS4*/*GAS4*[2 μm-*GAS2–URA3*]	10.3 ± 2.8	0.4 ± 0.2	5.4 ± 2.7	16.6 ± 2.7	67.3 ± 7.4
ER316	*GAS2*/*GAS2 GAS4*/*GAS4*[2 μm-*GAS4–URA3*]	8.5 ± 3.1	0	7.4 ± 1.8	14 ± 1.8	70.1 ± 3.7
Tagged *GAS2* gene[c]						
ER317	*gas2*Δ *gas4*Δ/*gas2*Δ *gas4*Δ[2 μm-*URA3*]	69.9 ± 12.1	8.8 ± 4.4	9.8 ± 4.1	7.9 ± 3.2	3.6 ± 1.2
ER313	*gas2*Δ *gas4*Δ/*gas2*Δ *gas4*Δ[2 μm-*GAS2–URA3*]	19 ± 7.4	0.6 ± 0.3	8.1 ± 1.6	18.3 ± 6.2	54 ± 13.5
ER315	*gas2*Δ *gas4*Δ/*gas2*Δ *gas4*Δ[2 μm-*GAS2*-3xHA–*URA3*]	18.7 ± 10.3	0.9 ± 0.5	8.5 ± 0.6	15.2 ± 2.1	56.7 ± 12.4

[a] The values are the means ± standard deviations of three independent experiments. Totals of 200 cells of the indicated strains were analyzed by phase-contrast microscopy after 24 h in sporulation medium.
[b] The indicated strains were grown in YPA and sporulated in SPM-1.
[c] The cells were grown in SA and were analyzed 24 h after the shift to SPM-2.
[d] For this strain, spore edges were not easily distinguished. Cells were counted as sporulated cells when at least one spore was visible or spores edges were defined.

GAS2 and *GAS4* transcripts were not detectable at time zero, suggesting that these genes are not substantially transcribed in cells growing in presporulation medium (YPA).

These data are in agreement with the microarray analysis of sporulating yeast cells that showed that *GAS2* and *GAS4* are strongly induced during the middle phase of sporulation, leading them to be classified in cluster 5a of the middle genes (7, 38). However, the microarray analysis was limited to the first 11.5 h of the sporulation process, while our study extends the analysis to the completion of the sporulation process.

Gas2 and Gas4 protein levels during sporulation. The levels of Gas2 and Gas4 proteins during sporulation were monitored. To detect Gas2p, a tagged version of the protein was constructed, whereas for Gas4p, a polyclonal antiserum raised against the recombinant form of Gas4p was used. Since *GAS2*'s sequence predicts a polypeptide that has a signal peptide at the N-terminal end and the GPI attachment signal at the C-terminal end, the tag was inserted internally. To construct a fusion that did not affect the function of the protein, the Gas2 protein sequence was first analyzed with the GlobPlot 2 method that predicts the globular and disordered regions of a protein (29). The 3 × HA tag was inserted in a C-terminal random coil segment of the protein between residues S509 and N510. Then, the fused gene was cloned in a multicopy plasmid. To first verify that overexpression of the untagged *GAS2* gene did not bring about any detrimental effect on sporulation, the *GAS2* gene was introduced into the SK1 strain in a high-copy-number plasmid, generating the strain ER311. Overexpression of *GAS2* had no relevant effect on sporulation compared to the SK1 strain harboring the empty vector and named ER310 (Table 3). Then, to check if the tagged version of the *GAS2* gene was functional, the modified gene was introduced into the double *gas2 gas4* null diploid mutant, generating the strain ER315. Whereas the single *gas2*Δ or *gas4*Δ mutants have no change in their sporulation phenotypes, the double *gas2*Δ/*gas2*Δ *gas4*Δ/*gas4*Δ mutant was severely defective (see below for more details). As shown in Table 3, the tagged *GAS2* gene fully reversed the defective phenotype of the *gas2 gas4* null mutant, since the percentage of unsporulated cells was approximately 19% compared to about 70% for the double mutant transformed with the empty vector (ER317). Moreover, the percentages of mature asci with four spores were very similar between the strains transformed with the *GAS2* gene and with the tagged version (Table 3). Therefore, we concluded that the tagged protein was functional. The plasmid YER-2-HA harboring the tagged gene was introduced also into a *gas2*Δ/*gas2*Δ mutant, and the resulting strain (ER314) was used for the time course experiment. At different time intervals from the induction of sporulation, total protein extracts were prepared and analyzed by immunoblotting using anti-HA, anti-Gas4p, and anti-actin antibodies (Fig. 2A). Consistent with the gene expression profile, the Gas2-3xHA protein was undetectable at time zero and started to be detectable at 6 h as a major, 64-kDa polypeptide (Fig. 2A). Levels of the 64-kDa polypeptide increased, reaching a maximum at 8 h before gradually decreasing (Fig. 2B, upper panel). A lower band of ~60 kDa was also detected at the time of maximal expression (Fig. 2A). It may represent an intermediate precursor of the 64-kDa polypeptide that converts to the mature form over longer times.

The Gas4p levels were also consistent with the gene expression profile. The Gas4 protein appeared as a 54-kDa polypeptide that was undetectable at time zero and rapidly increased starting from 6 h, reaching a maximum at 10 h from transfer of the cells to SPM-2. After 10 h, the protein levels began to steadily decrease. The behavior of the Gas4p levels during sporulation is shown in Fig. 2B, lower panel. It was not influenced by overexpression of Gas2p, since the same profile was obtained in a time course experiment performed using the parental SK1 strain (data not shown). The specificity of the antiserum used was also checked. Gas4p was absent in sporulating *gas4*Δ/*gas4*Δ cells at the time of maximal expression (Fig. 2C, lane 1). Moreover, the serum recognized a 54-kDa band in haploid *gas1*Δ cells ectopically expressing *GAS4* (Fig. 2C, lane

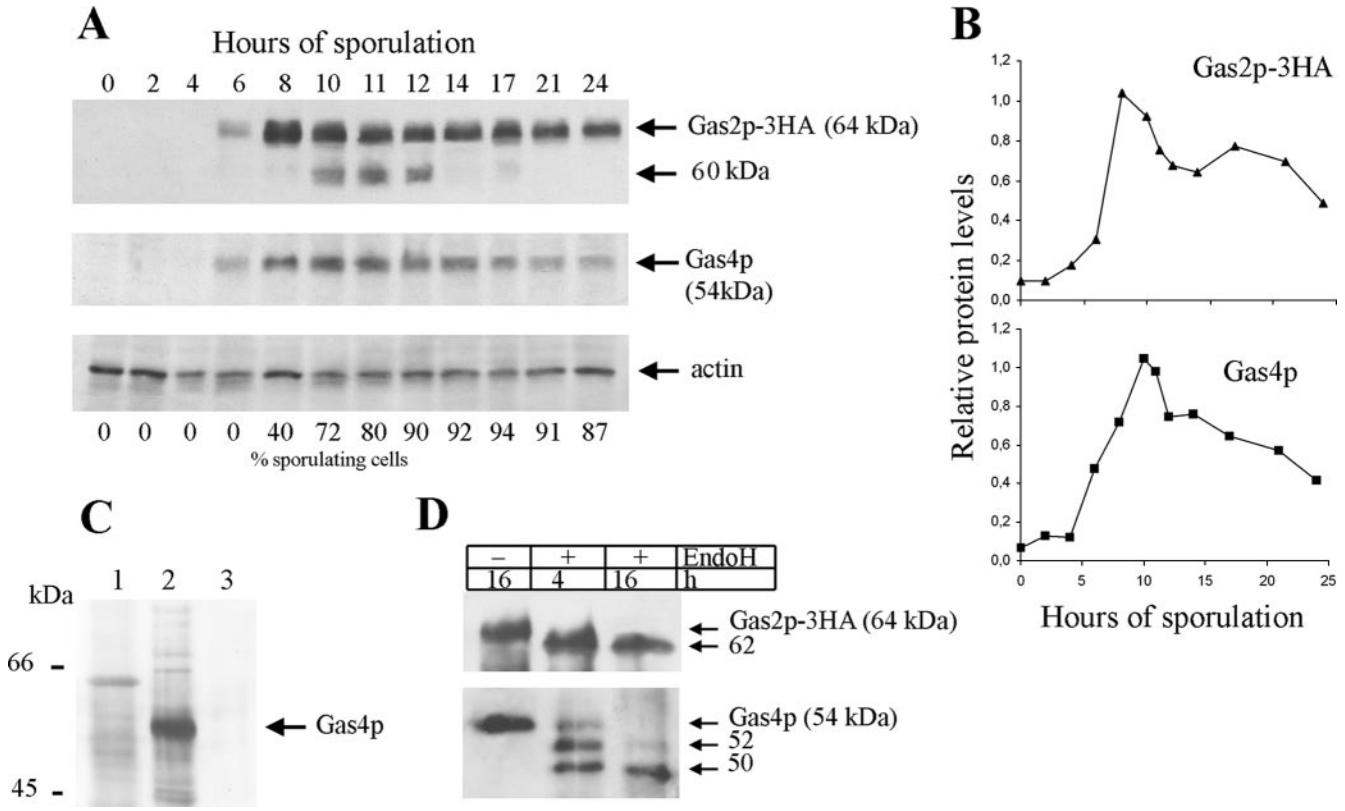

FIG. 2. Levels of Gas2p and Gas4p during sporulation. (A) Total protein extracts (60 μg) from sporulating cells were analyzed by immunoblotting using anti-HA (upper panel), anti-Gas4p (central panel), or anti-actin (lower panel) antibodies. (B) Gas2 and Gas4 protein levels are relative to the level of actin protein (42 kDa) used to normalize for the protein load in the same immunoblot. (C) Analysis of the specificity of anti-Gas4p serum. The following extracts were analyzed: total protein extract from the *gas4*Δ/*gas4*Δ strain at 10 h from sporulation (lane 1) and extracts from Y4 and Y0 strains growing exponentially in minimal medium at 30°C (lanes 2 and 3). (D) Glycosylation profiles of Gas2p and Gas4p. Protein extracts from strains overexpressing Gas2p3xHA (ER314) or Gas4p (ER316) were prepared at 24 h from induction of sporulation and were incubated with (+) or without (−) EndoH for the indicated time. Immunoblots with anti-HA monoclonal antibody or anti-Gas4p serum are shown.

2). This band was absent in the same cells transformed with the empty vector (Fig. 2C, lane 3).

The profile of Gas4p levels suggests that its regulation occurs not only at the transcription level, but also at the level of protein stability. Moreover, the apparent molecular mass of Gas4p appears higher than predicted for this polypeptide lacking the putative N- and C-terminal signal sequences (48,520 Da), suggesting that this protein is probably modified by glycosylation. Similarly, the predicted molecular mass of Gas2-3xHAp lacking the N- and C-terminal signal sequences is 60,600 Da, and therefore, Gas2p could also be modified. To verify if Gas2 and Gas4 proteins are glycosylated, total extracts from sporulating cells overexpressing these proteins were subjected to treatment with EndoH, an enzyme that removes N-linked chains. The effects of short (4 h) and long (16 h) incubations were analyzed (Fig. 2D). Gas2p showed a shift in mobility at 4 h, giving rise to a band of about 62 kDa. Its pattern of deglycosylation did not change at 16 h of treatment. This indicates that only one short N-linked chain is present, in agreement with the prediction of a single potential N-glycosylation site in Gas2p. At 4 h of treatment, Gas4p showed the reduction of the intensity of the 54-kDa band and the appearance of two lower bands, of ~52 and 50 kDa. At 16 h, only the 50-kDa band was present (Fig. 2D). This result indicates that two N-linked chains are attached to Gas4p and that the two potential N-glycosylation sites present in the sequence are both used in vivo.

Loss of *GAS2* and *GAS4* reduces the efficiency of sporulation. The effects of the loss of *GAS2* and *GAS4* genes were examined in two sporulation-proficient strains: W303 and SK1. The phenotypes of haploid *gas2*Δ, *gas4*Δ, and *gas2*Δ *gas4*Δ strains and of the corresponding homozygous null diploids were first examined during vegetative growth. In YPD at 30°C, the null mutations did not cause any obvious changes in the growth rates or in cell morphologies. Moreover, two phenotypic indexes of cell wall damage, calcofluor white sensitivity and activation of the cell integrity pathway, were unaffected (data not shown). Upon induction of sporulation, the diploid $W303^2$ strain completed sporulation in 48 h. At this time the percentages of sporulated cells, determined in three different experiments, were 73% for the wild type and 59%, 52%, and about 30% for the *gas2*/*gas2*, *gas4*/*gas4*, and *gas2 gas4*/*gas2 gas4* mutants, respectively, taking into account that in the double null mutant, detection of the spores was difficult. Remarkably, at 48 h, mature asci with 4 spores represented 50% of the total cells in the parental strain, whereas they represented only 15%, 16%, and 5%, respectively, of the total cells in the mutants, suggesting that the defect in spore maturation was present in

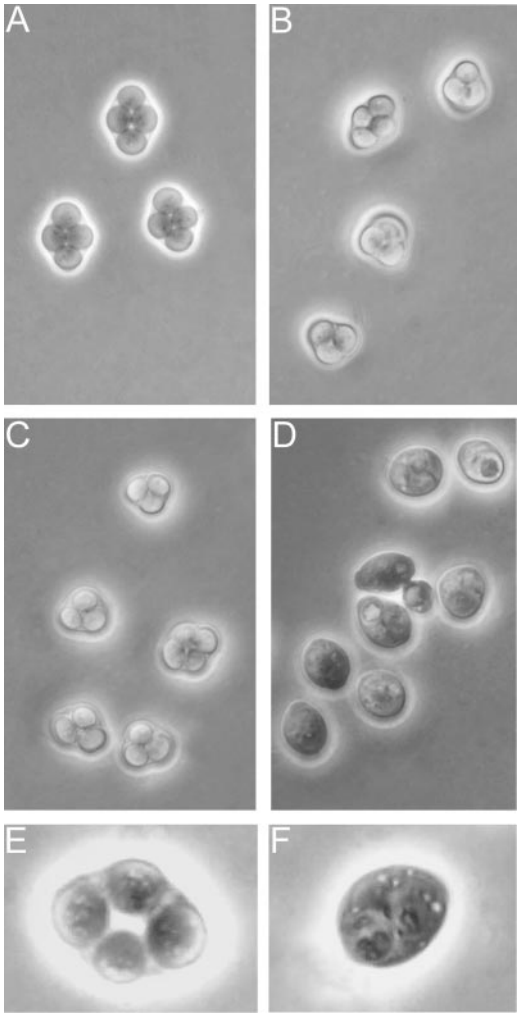

FIG. 3. Cell morphologies in *gas* mutants under sporulating conditions. Cells were observed with phase-contrast microscopy after 24 h of sporulation. The panels show wild-type (SK1) cells (A), *gas2*Δ *gas2*Δ mutant cells (B), *gas4*Δ *gas4*Δ mutant cells (C), *gas2*Δ *gas4*Δ/*gas2*Δ *gas4*Δ mutant cells (D), detail of a wild-type ascus (E), and detail of a *gas2*Δ *gas4*Δ/*gas2*Δ *gas4*Δ mutant ascus (F) (see text).

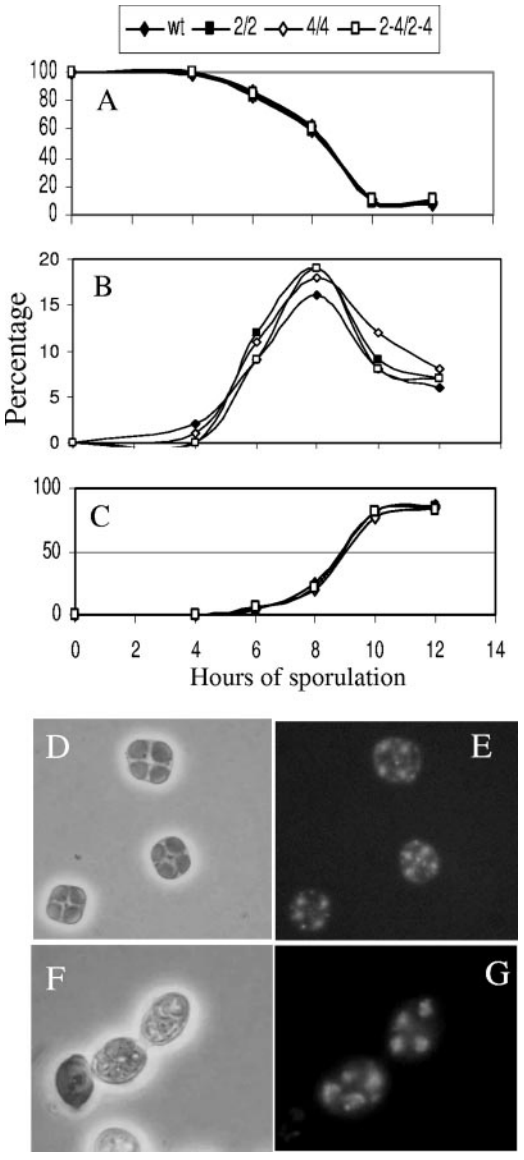

FIG. 4. Kinetics of the progression of meiosis in *gas2*, *gas4*, and *gas2 gas4* diploid null mutants. Cells were stained with DAPI at different time intervals during sporulation and examined by fluorescence microscopy. The percentages of mononucleate (A), binucleate (B), and tetranucleate (C) cells were determined. Panels D and F show the morphologies of asci of the wild type (D) and the *gas2 gas4* double null mutant (F) examined under white light, and panels E and G show the same cells observed under fluorescence microscopy.

the single mutants and became worse in the absence of both genes. Next, we verified the behavior of the homozygous null mutants during sporulation in the SK1 genetic background. As reported in Table 3, at 24 h the percentage of unsporulated cells was not appreciably affected in the *gas2*Δ/*gas2*Δ and *gas4*Δ/*gas4*Δ mutants with respect to the parental strain, whereas it increased in the *gas2*Δ *gas4*Δ/*gas2*Δ *gas4*Δ mutant. Moreover, mature asci with 4 spores were only 0.7% of the total cells in the double mutant, compared to 65 to 70% of the total cells in the parental strain and in the single mutants (Table 3). The lack of clear definition of spore edges made the determination of ascal type in the double mutant difficult (see below). However, a marked increase in the numbers of monads and triads was observed. In conclusion, the mutations affect sporulation similarly in W303[2] and SK1 strains, but the single *gas2* or *gas4* null mutations display greater changes in phenotype in W303[2] than in SK1.

The morphologies of sporulating SK1-derived cells are shown in the phase-contrast micrographs of Fig. 3. As shown in panels B and C, the spores of the single mutants were round and arranged in a regular fashion, like the control (panel A), and were bright. In the double mutant (panel D), cells appeared less bright and refractile, the internal separation of the cytoplasm was unclear, and many granules were present. Moreover, the scoring of sporulated cells was difficult since spore edges were not clearly visible or appeared thin. A detail of this phenotypic trait is shown in Fig. 3F. Cells with one spore of normal size close to a small one were also frequent (about 15% of the total). Thus, the double mutation causes severe

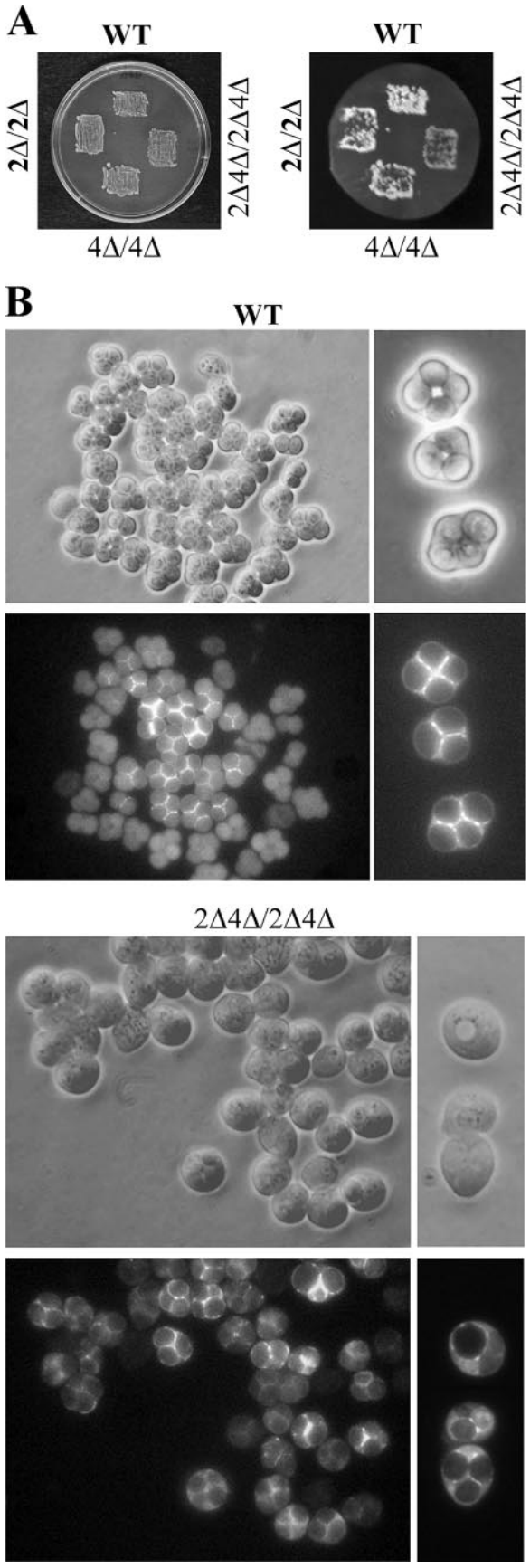

defects in spore formation and maturation, giving origin to a heterotypic phenotype. The morphologies of sporulating W303-derivative strains were very similar to those described above for SK1 strains (data not shown). Since in both strains the reduction of the efficiency of spore formation in the double mutant is more severe than in the single mutants, *GAS2* and *GAS4* genes play a partial, redundant role in sporulation. Due to its higher degree of synchrony in sporulation, further analysis of spore wall defects was carried out only for SK1-derived mutants.

The effects of overexpression of *GAS2* and *GAS4* were tested by analyzing SK1 strains carrying these genes on a multicopy plasmid (ER311 and ER316 strains). As shown in Table 3, no appreciable effects on sporulation efficiency were observed compared to that of the isogenic strain transformed with the empty vector (ER310), indicating that neither *GAS2* nor *GAS4* is detrimental for sporulation when overexpressed.

Nuclear progression occurs normally in the *gas2* and *gas4* mutants. In order to determine if the loss of *GAS2* and *GAS4* genes primarily affected the meiotic process and the effect on spore morphogenesis was a consequence of this defect, the kinetics of chromosomal segregation in the mutants was monitored by nuclear DNA staining of cells undergoing sporulation. The results are shown in Fig. 4A to C. The kinetics of formation of cells with 1, 2, or 4 nuclei were not significantly affected by the mutations. Moreover, very similar percentages of tetranucleate cells were reached at 12 h from sporulation induction. Thus, meiotic progression does not appear to be significantly affected by the lack of *GAS2* or *GAS4* or both *GAS2* and *GAS4*. Cells stained by DAPI are shown in Fig. 4D to G. Panels F and G show examples of double-mutant cells in which spores were not clearly distinguished, but four nuclei were present. We can conclude that Gas2 and Gas4 proteins are not required for meiotic progression.

Deletion of *GAS2* and *GAS4* leads to spore wall-defective phenotypes. Further evidence for defects in spore formation was obtained by analyzing the presence of dityrosine, a specific component of the outermost layer of the spore wall. A qualitative assay that exploits the fluorescence of dityrosine under UV light was performed as described in Materials and Methods. Patches of the parental and mutant strains were replica plated on a nitrocellulose filter and placed on solid sporulation medium. After 3 days, the filters were observed. As shown in Fig. 5A, the fluorescence observed for the *gas2 gas4* null mutant was less intense than for the other strains. This indicates that dityrosine is present but less abundant, consistent with the low efficiency of sporulation of the double mutant. Cells undergoing sporulation in liquid medium were also analyzed with the microscope under conditions of basic pH that enhance the dityrosine fluorescence. Surprisingly, in the double mutant,

FIG. 5. Qualitative assay of dityrosine and microscopic analysis of intact asci. (A) Patches of cells of the indicated diploid strains were grown on a YPD plate, photographed (left panel), replica plated onto a nitrocellulose filter, and again photographed under UV light after 3 days on a sporulation plate (right panel). (B) SK1 (WT) and *gas2 gas4* null mutant cells were collected at 24 h after induction of sporulation and visualized both with phase-contrast microscopy (upper panels) and under UV light (lower panels) after resuspension in 5% aqueous ammonia. Details are shown in the right panels.

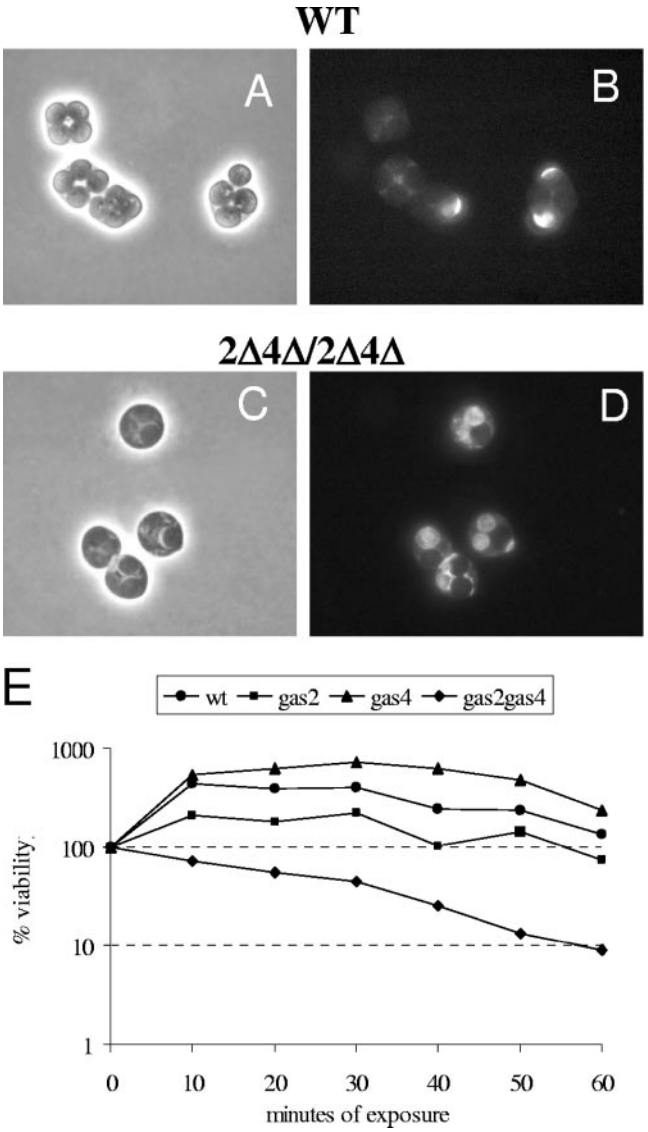

FIG. 6. Results of permeability assays. Wild-type (A and B) and *gas2*Δ *gas4*Δ/*gas2*Δ *gas4*Δ mutant (C and D) cells were stained with calcofluor white and visualized by white-light microscopy (A and C) and fluorescence microscopy (B and D) at 24 h of sporulation. (E) Cells of the different strains were exposed to Zymolyase for the indicated times and then plated on rich medium to determine the titers of viable cells. For each strain, viability is expressed as the percentage of viable cells present at time zero (100%).

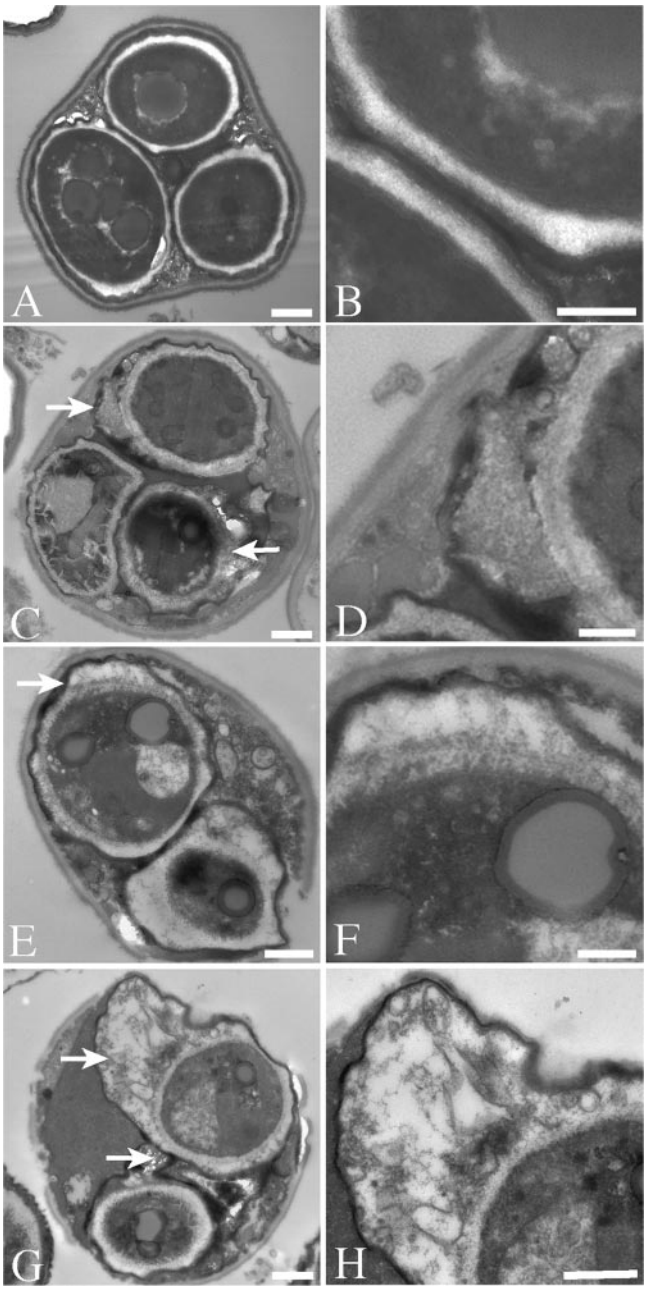

FIG. 7. Ultrastructure of the spore wall in the *gas2*Δ *gas4*Δ/*gas2*Δ *gas4*Δ mutant. The panels show TEM analyses of spores in wild-type (A and B) and *gas2*Δ *gas4*Δ/*gas2*Δ *gas4*Δ (C to H) cells. Panels B, D, F, and H show higher-magnification images of sections of the spore wall in the cells shown in panels A, C, E, and G, respectively. Arrows indicate sites of accumulation of disordered material. Bars, 500 nm (A, C, E, and G) and 200 nm (B, D, F, and H).

microscopic examination of dityrosine revealed the presence of spores that were not detectable with phase-contrast microscopy (Fig. 5B), even though the number of spores per ascus was lower than for the wild type and their shape was irregular. At closer examination of the wild type, the asci showed a regular arrangement of fluorescence with a brighter signal at the contact points between spores (Fig. 5, details in the micrograph on the right). In the double mutant, the dityrosine was less regularly arranged and was also found diffusely throughout the ascus. Cells negative for dityrosine were also present. (Fig. 5, see details on the right). Thus, the double mutant seems to be defective in the normal accumulation and deposition of the dityrosine layer.

Intact cells undergoing sporulation were stained with CW, a dye that binds to chitin or chitosan fibrils but is also an indicator of defects in permeability (16). Cells with defects in spore wall assembly become permeable to this dye that otherwise would not penetrate into intact cells (34). As shown in Fig. 6A and B, in the parental cells bright areas corresponding to bud

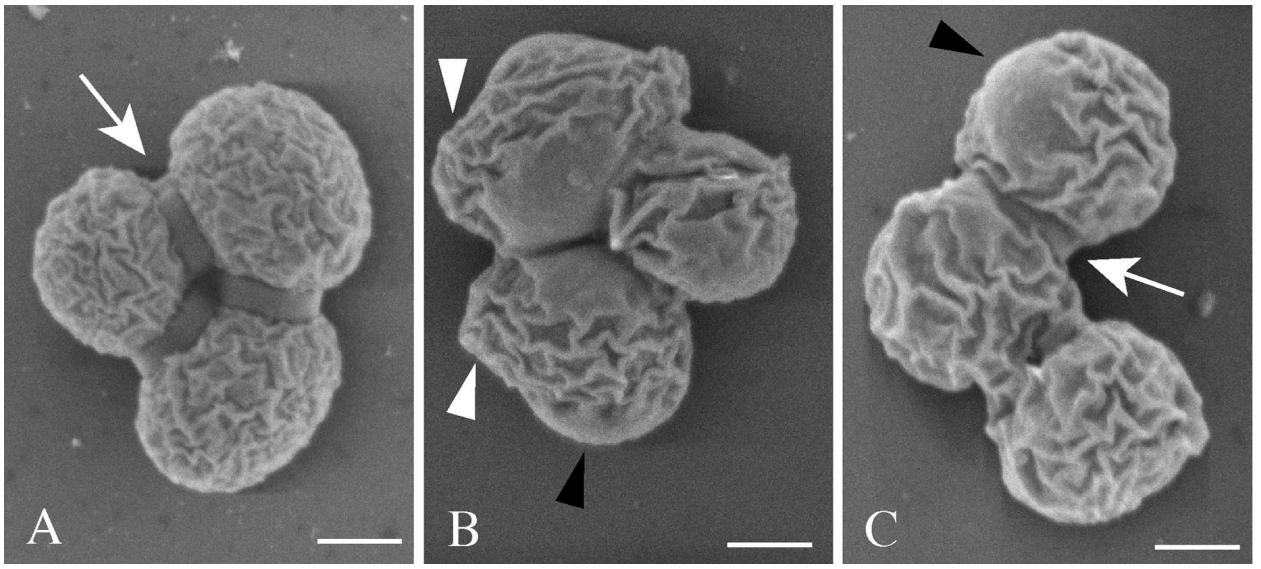

FIG. 8. SEM analysis. The panels show SEM images of spores from wild-type (A) and *gas2*Δ *gas4*Δ mutant (B and C) cells. Arrows indicate interspore bridges, white arrowheads indicate regions where the spore wall is distended on the *gas2*Δ *gas4*Δ mutant spores, and black arrowheads indicate smooth surface regions on the *gas2*Δ *gas4*Δ mutant cells. Bars, 1 μm.

scars of the mother cell are detected, whereas a faint internal staining of the spore edges corresponding to the chitosan layer is also visible. In the *gas2 gas4*/*gas2 gas4* mutant, CW stains some spores internally, indicating that severe permeability defects or dead spores are present inside the asci (Fig. 6C and D). This staining of spores was not detected in the single mutants, which resembled the wild type (data not shown). In order to quantify this defect, we exploited a viability assay using Zymolyase. Zymolyase hydrolyzes the β(1,3)-glucan layer of the ascus wall and releases the spores but is not able to attack the glucan layer of the spore wall, since the chitosan and dityrosine layers limit its accessibility. Thus, the loss of the capability to form colonies after Zymolyase treatment is an index of increased spore wall permeability to Zymolyase. We performed a quantitative assay of the Zymolyase sensitivity of sporulated cells at 24 h from induction of sporulation. The results are shown in Fig. 6E. The CFU values at different times after exposure to Zymolyase were compared to the value at time zero for each strain. As shown, the wild-type cells and *gas2* and *gas4* null diploid mutants released spores that were still viable after longer times of treatment, whereas the viability of the *gas2 gas4* double mutant cells steadily decreased, reaching a 10-fold drop in viability after 1 h of incubation. Moreover, the absolute CFU values at time zero were about four times lower for the double mutants than for the parental and single mutant cells. The number of CFU obtained from 10^5 sporulating cells was about 4.5×10^4 for the single mutant and parental strains and about 1.1×10^4 for the double mutant. These results indicate that double mutant cells were less viable even in the absence of Zymolyase. In conclusion, defects in *gas2*Δ *gas4*Δ spore formation lead to a lowered viability and a higher permeability to the uptake of exogenous molecules into the spores.

TABLE 4. Effects of the ectopic expression of *GAS2* and *GAS4* on the growth of the *gas1*Δ mutant at different pH values

Strain	Growth rate [μ (h^{-1})][a]		
	Unbuffered medium	Buffered medium (pH 5.5)	Buffered medium (pH 6.5)
W303-1B	0.54	0.55	0.48
WB2d (*gas1*Δ)	0.32	0.30	0.16
Y0	0.34	0.35	0.17
Y1	0.51	0.46	0.43
Y2	0.23	0.26	0.33
Y4	0.31	0.42	0.40

[a] Growth was measured as the increase in OD_{450}. Values are the means of three independent experiments. The pH of the buffered medium during growth never changed by more than 0.1 unit.

Cell wall ultrastructure. To further characterize the spore wall defect in *gas2 gas4* cells, the ultrastructure of the spore wall was examined by both transmission and scanning electron microscopy. TEM analysis suggests that all four of the layers of the spore wall are present and the outer chitosan and dityrosine layers appear to be intact (Fig. 7). However, frequent defects are seen at the interface between the β-glucan and chitosan layers (Fig. 7). At these sites, the β-glucan and chitosan layers are dissociated and an accumulation of disordered material, possibly unassembled carbohydrate chains, is seen. This accumulation results in a protrusion of the outer layers of the spore wall.

The appearance of the *gas2 gas4* spores under SEM is consistent with the TEM results (Fig. 8). The surface texture of the spores appears similar to that of the wild type, and interspore bridges are present, suggesting that the assembly of the outer chitosan and dityrosine layers is largely normal. However, the spores often appear misshapen, with prominent bulges as well as extended areas of the surface that appear flat, rather than scalloped as in wild-type spores (Fig. 8). These bulging and flattened areas may correspond to the accumulations of material at the β-glucan–chitosan interface seen under TEM. In sum, the ultrastructural analysis of *gas2 gas4* spores suggests

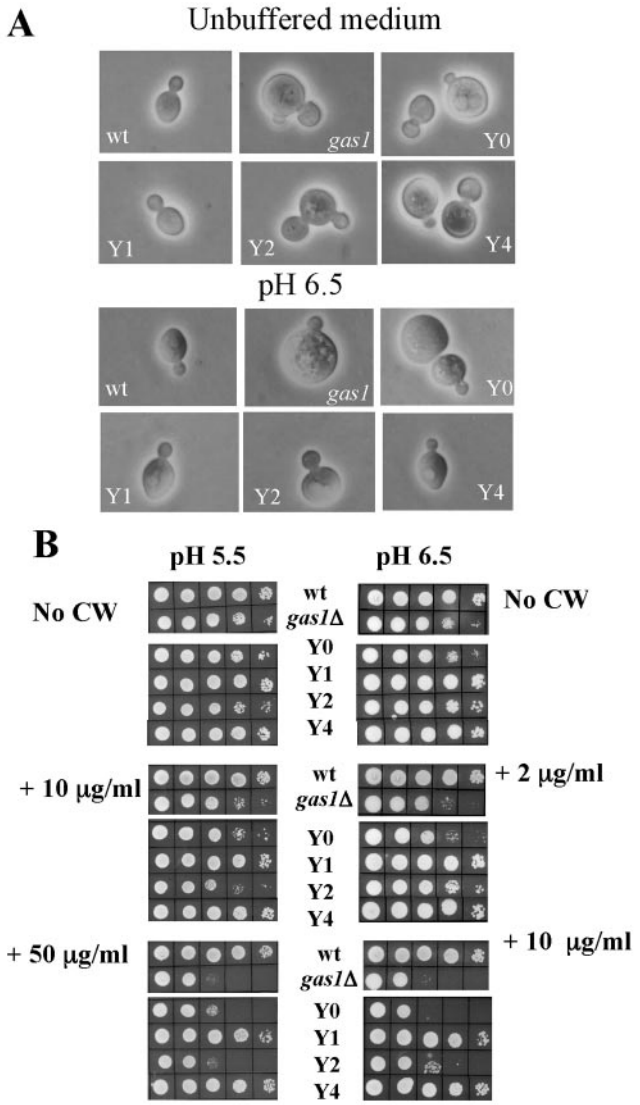

FIG. 9. Analysis of complementation of the *gas1*Δ mutant phenotype by ectopically expressed *GAS2* and *GAS4* genes. (A) Cells of the indicated strains were observed with phase-contrast microscopy during the exponential growth phase. (B) CW sensitivities of the indicated strains. CW concentrations in the plates are indicated on the sides. wt, wild type.

that the mutant is defective in attachment of the inner and outer spore wall layers to each other. This results in spores that have improperly organized, less-robust walls, consistent with the poor refractility of the spores under the light microscope (see Discussion).

Does ectopic expression of *GAS2* and *GAS4* complement the *gas1* null mutant phenotype? The ability of *GAS2* and *GAS4* to complement the *gas1* null mutant phenotype was examined. In order to allow the expression of these genes in vegetative growth, their promoter was replaced with the *GAS1* promoter (P_{GAS1}). The YEp24 vector and recombinant YEp24 plasmids harboring the *GAS1* gene, P_{GAS1}-*GAS2* or P_{GAS1}-*GAS4*, were used to transform a *gas1* null mutant. The resulting transformants were named Y0 (vector), Y1 (YEp24-*GAS1*), Y2 (YEp24-P_{GAS1}-*GAS2*), and Y4 (YEp24-P_{GAS1}-*GAS4*). The kinetics of growth were monitored, and in Table 4, the values of the growth rate (μ) are shown. Interestingly, the growth rates of Y2 and Y4 were the same as those of the Y0 and *gas1*Δ strains, indicating that no complementation occurred in SD medium (Table 4). This was confirmed by the analysis of cell morphology (Fig. 9A). We reasoned that spore walls develop in an intracellular compartment and, thus, the pH of the environment in which Gas2p and Gas4p normally function could be close to neutrality. Cells acidify the medium during growth, and indeed, the pH of the SD medium was found to be about 3.5 at mid-exponential phase. Therefore, we tested the effect of buffering the medium to pH values of 5.5 and 6.5 on the suppression of the *gas1*Δ phenotype by *GAS2* and *GAS4* genes. As shown in Table 4, *GAS4* suppressed the mutant phenotype partially at pH 5.5 and almost fully at pH 6.5. At the latter pH value, the swollen-cell morphology typical of *gas1* cells, which is exacerbated by the increased pH, was totally suppressed and cells appeared similar to wild-type cells (Fig. 9A). At pH 5.5, the *GAS2* gene did not complement the *gas1*Δ phenotype, as the Y2 strain has a growth rate lower than that of Y0, and its morphology appeared slightly worse than that of *gas1*. At pH 6.5, the phenotypic defects of the *gas1*Δ strain were partially reversed, since the Y2 cells grew slightly faster and the cells were smaller than *gas1*Δ mutant cells but still rounder than wild-type cells (Table 4 and Fig. 9A). The effect on *gas1* mutant cells of buffering the medium to pH 6.5 was further analyzed by monitoring the suppression of hypersensitivity to CW, another phenotypic trait typical of *gas1* mutant cells. In Fig. 9B, it is possible to observe that *GAS2* did not suppress the hypersensitivity of *gas1* cells to CW at pH 5.5. At pH 6.5, the suppression of hypersensitivity to CW by *GAS2* was only partial, as shown by the plates containing 2 μg/ml of CW, and cells were still hypersensitive at higher concentrations of CW (Fig. 9B). On the other hand, *GAS4* complemented CW hypersensitivity at both pH 5.5 and 6.5 (Fig. 9B). Altogether, the data indicate that both Gas2p and Gas4p are functional homologs of Gas1p, but Gas4p replaces Gas1p function better than Gas2p. Gas2p partially complements the *gas1*Δ phenotype only at pH 6.5.

DISCUSSION

The *GAS* gene family of *S. cerevisiae* is composed of the well-studied *GAS1* gene and four paralogs (*GAS2* to *GAS5*) that have never been investigated. This study addressed the roles of two of the paralogues, *GAS2* and *GAS4*. Whereas *GAS1* is expressed in vegetative growth and its transcription is shut down as cells enter sporulation (7, 34, 38), the *GAS2* and *GAS4* genes exhibit the reverse behavior (7, 38). The expression of *GAS2* and *GAS4* is triggered in cells undergoing sporulation and is absent during vegetative growth. In particular, we have shown in this work that *GAS2* and *GAS4* mRNA levels increase rapidly and reach a maximum at 7 h from the induction of sporulation and afterwards they start to decline. The time of maximal expression is coincident with the stage of sporulation in which the spore wall is formed (7). The *GAS2* and *GAS4* gene expression profiles are in agreement with the

presence of MSE elements in the promoter regions of these genes. A strong match to the MSE site consensus (5′HDVKN CACAAAAD) was found in the *GAS4* promoter at positions −117 to −105 (5′GCGGCACAAAAA) from the ATG, whereas a less stringent match (5′DNCRCAAAWD) was detected in the *GAS2* promoter in the reverse orientation at positions −147 to −138 (5′GACACAAATT) from the start codon. The presence of a more stringent match in the *GAS4* promoter could explain the higher expression level of *GAS4* with respect to *GAS2*, since Ndt80p, the transcription factor that binds the MSE element, might recognize it with higher affinity. Ndt80p is the major regulator of the middle meiotic class of genes in which *GAS2* and *GAS4* were classified (7). Microarray analysis revealed that Ndt80p itself has an expression profile very similar to those of *GAS2* and *GAS4* and is the main candidate for the temporal regulation of *GAS2* and *GAS4* expression. Indeed, the ectopic expression of Ndt80p in vegetative cells triggers the expression of *GAS2* and *GAS4* and the lack of Ndt80p almost completely abolishes the expression of *GAS2* and *GAS4* during sporulation (7). The induction of *GAS2* and *GAS4* gene expression might also involve a change in chromatin organization. Microarray analysis of vegetatively growing cells indicated that *GAS2* and *GAS4* are among the genes that are normally transcriptionally silent and become induced by histone H4 depletion (44). Thus, Ndt80p, modifications of the chromatin, and nucleosome density could all be relevant for the regulation of the expression of *GAS2* and *GAS4* genes.

In this study, we found that Gas2p and Gas4p levels show maximums at 8 and 10 h, respectively. In particular, the level of Gas4p starts to decline slowly after 10 h from the induction of sporulation. The boost of *GAS4* mRNA production in a narrow window of the sporulation process could be crucial to attain the required level of protein. After the execution of the protein's function, the decrease in the protein level would result from the reduction of transcription and lability of the protein. An alternative hypothesis is that a degradation mechanism specific for the Gas4 protein is triggered after Gas4p has completed its function. In both cases, the degradation of Gas4 protein, and maybe of other proteins involved in cell wall formation, could be a physiological response aimed at making amino acids available for the synthesis of late-sporulation products under conditions in which no exogenous nitrogen source is present and no net synthesis of amino acids occurs. Gas2p appears more stable, and its final localization could be the spore wall, based on the absence of a dibasic motif upstream of the GPI attachment site (5, 27). Further studies aimed at analyzing the localization of Gas2 and Gas4 proteins are under way.

The results of the phenotypic analysis of deletion mutants support a role for *GAS2* and *GAS4* gene products in spore wall assembly. A severe defect was observed only when the deletions of *GAS2* and *GAS4* were combined. Thus, the two genes share overlapping functions. Because the phenotype is most clearly seen when both genes are inactivated, *GAS2* and *GAS4* genes escaped the previous screening of a library of single diploid mutants (8).

The effects of the loss of Gas2 and Gas4 proteins on spore wall morphogenesis are dramatic. Synthesis of all the layers of the spore cell wall occurs, but the accumulation of wall material is abnormal. The connection of the β-glucan and the overlying chitosan layer appears to be defective. However, this effect might simply be a consequence of the lack of coherence of the inner layer. Since Gas2 and Gas4 proteins are endowed with β(1,3)-glucanosyltransferase activity similar to that of Gas1p (unpublished data), the double mutant might have shorter β(1,3)-glucan chains in the inner layer of the spore wall. Thus, the connection of chitosan to a less compact glucan network could make the spore wall more fragile and easily stripped under harsh conditions, as the TEM analysis indicates. These defects cause an increase in spore permeability to exogenous substances, a decrease in refractivity, and a marked decrease in spore viability. Interestingly, this phenotype is similar to the phenotype described for mutants lacking the *CRR1* gene encoding a putative sporulation-specific transglycosidase that is probably directly involved in the connection of glucans to the chitosan layer (16). With regard to the recently proposed morphogenetic pathway of spore wall formation (33), the possible execution point for *GAS2* and *GAS4* could be between the synthesis and organization of β(1,3)-glucan and, more specifically, in the elongation of the β(1,3)-glucan chains. Other mutants with defects at this point, such as *sps2 sps22*, which are defective in genes encoding putative GPI-anchored cell proteins, do not block the process of wall assembly, but the assembly is compromised, and the spores do not acquire a functional spore wall (8). As mentioned before, both Gas2 and Gas4 proteins contain a C-terminal signal for GPI attachment. Their involvement in sporulation can partially explain the severe sporulation phenotype of *gpi* diploid mutants, defective in the first step of GPI anchor assembly (26). However, since dityrosine is not present in *gpi* mutants, other GPI proteins besides Gas2p and Gas4p might contribute to such a severe sporulation phenotype.

GAS2 and *GAS4* are regulated differently from *GAS1*, but do their products have the same function as Gas1p? To answer this question, we ectopically expressed *GAS2* and *GAS4* in a *gas1* null mutant and examined the phenotype during vegetative growth. Interestingly, Gas4p was found to complement the mutant phenotype of *gas1* almost fully at a pH of 5.5 and fully at higher pH values. Gas2p is able to partially complement the mutant phenotype only at pH 6.5 and not as efficiently as Gas4p. The pH dependence in the ability of Gas2p and Gas4p to replace Gas1p points to several factors, such as a different optimal pH of the two enzymes with respect to Gas1p; an effect of pH on cell wall organization, in agreement with previous reports (20); and effects on microenvironmental conditions, on interactions with other cell wall proteins, and on mechanisms of protein transport and localization. It should be noted that, unlike the cell wall, the spore wall is assembled initially in an intracellular membrane-bound compartment. Though the pH of this compartment is not known, it is likely to be close to neutral. Moreover, during the process of spore wall assembly, the outer membrane derived from the prospore membrane breaks down, exposing the spore wall proteins to the ascal cytoplasm, which is likely to have a neutral pH. Finally, it has been shown that upon entry into sporulation, yeast cells alkalinize the medium, with optimum sporulation occurring around pH 7 to 8 (26). All of these observations suggest that the apparent preference of Gas2 and Gas4 for a higher pH may

reflect the in vivo conditions under which these proteins normally function.

In addition to the *GAS* family, several other secreted proteins involved in cell wall assembly have sporulation-specific paralogs in *S. cerevisiae* (5, 12, 25). The behavior shown by Gas2 and Gas4 proteins in the ectopic expression experiments suggests a novel explanation for the existence of redundant families of enzymes involved in cell wall formation. Not only the different organization of the spore wall but the different environments in which the cell wall and spore wall are formed could have driven the evolution of sporulation-specific paralogs specialized to function optimally at different pH values. In this regard, future studies on the paralogous enzymes will be crucial for understanding the roles of the different members of the gene families involved in spore wall formation.

ACKNOWLEDGMENTS

The work in the Popolo Lab was partially supported by Fondo Interno Ricerca Scientifica e Tecnologica 2004-2005, COFIN 2005, and the Cantrain project (MRTN-CT-2004-512481) of the European Union to L.P. The work in the Neiman lab was partially supported by NIH grant GM72540 to A.M.N. and that in the Arroyo lab by project BIO2004-06376 from the Ministerio de Educacion y Ciencia to J.A.

We thank M. Vai for the kind gift of plasmids, Michela Pacei for technical assistance, and Rosa M. Perez-Díaz and J. García-Cantalejo from the Unidad de Genomica UCM-PCM for their help with the quantitative RT-PCR experiments.

REFERENCES

1. **An, Y., J. Ji, W. Wu, A. Lv, R. Huang, and Y. Wei.** 2005. A rapid and efficient method for multiple-site mutagenesis with a modified overlap extension PCR. Appl. Microbiol. Biotechnol. **68:**774–778.
2. **Boorsma, A., H. de Nobel, B. ter Riet, B. Bargmann, S. Brul, K. J. Hellingwerf, and F. M. Klis.** 2004. Characterization of the transcriptional response to cell wall stress in Saccharomyces cerevisiae. Yeast **21:**413–427.
3. **Briza, P., M. Breitenbach, A. Ellinger, and J. Segall.** 1990. Isolation of two developmentally regulated genes involved in spore wall maturation in Saccharomyces cerevisiae. Genes Dev. **4:**1775–1789.
4. **Briza, P., G. Winkler, H. Kalchhauser, and M. Breitenbach.** 1986. Dityrosine is a prominent component of the yeast ascospore wall. A proof of its structure. J. Biol. Chem. **261:**4288–4294.
5. **Caro, L. H., H. Tettelin, J. H. Vossen, A. F. Ram, H. van den Ende, and F. M. Klis.** 1997. In silicio identification of glycosyl-phosphatidylinositol-anchored plasma-membrane and cell wall proteins of Saccharomyces cerevisiae. Yeast **13:**1477–1489.
6. **Carotti, C., E. Ragni, O. Palomares, T. Fontaine, G. Tedeschi, R. Rodriguez, J. P. Latge, M. Vai, and L. Popolo.** 2004. Characterization of recombinant forms of the yeast Gas1 protein and identification of residues essential for glucanosyltransferase activity and folding. Eur. J. Biochem. **271:**3635–3645.
7. **Chu, S., J. DeRisi, M. Eisen, J. Mulholland, D. Botstein, P. O. Brown, and I. Herskowitz.** 1998. The transcriptional program of sporulation in budding yeast. Science **282:**699–705.
8. **Coluccio, A., E. Bogengruber, M. N. Conrad, M. E. Dresser, P. Briza, and A. M. Neiman.** 2004. Morphogenetic pathway of spore wall assembly in *Saccharomyces cerevisiae*. Eukaryot. Cell **3:**1464–1475.
9. **Coluccio, A., and A. M. Neiman.** 2004. Interspore bridges: a new feature of the Saccharomyces cerevisiae spore wall. Microbiology **150:**3189–3196.
10. **De Groot, P. W., A. F. Ram, and F. M. Klis.** 2005. Features and functions of covalently linked proteins in fungal cell walls. Fungal Genet. Biol. **42:**657–675.
11. **Douglas, C. M., F. Foor, J. A. Marrinan, N. Morin, J. B. Nielsen, A. M. Dahl, P. Mazur, W. Baginsky, W. Li, M. el-Sherbeini, et al.** 1994. The Saccharomyces cerevisiae FKS1 (ETG1) gene encodes an integral membrane protein which is a subunit of 1,3-beta-D-glucan synthase. Proc. Natl. Acad. Sci. USA **91:**12907–12911.
12. **Ecker, M., R. Deutzmann, L. Lehle, V. Mrsa, and W. Tanner.** 2006. Pir proteins of Saccharomyces cerevisiae are attached to beta-1,3-glucan by a new protein-carbohydrate linkage. J. Biol. Chem. **281:**11523–11529.
13. **Firon, A., G. Lesage, and H. Bussey.** 2004. Integrative studies put cell wall synthesis on the yeast functional map. Curr. Opin. Microbiol. **7:**617–623.
14. **Garcia, R., C. Bermejo, C. Grau, R. Perez, J. M. Rodriguez-Pena, J. Francois, C. Nombela, and J. Arroyo.** 2004. The global transcriptional response to transient cell wall damage in Saccharomyces cerevisiae and its regulation by the cell integrity signaling pathway. J. Biol. Chem. **279:**15183–15195.
15. **Gatti, E., L. Popolo, M. Vai, N. Rota, and L. Alberghina.** 1994. O-linked oligosaccharides in yeast glycosyl phosphatidylinositol-anchored protein gp115 are clustered in a serine-rich region not essential for its function. J. Biol. Chem. **269:**19695–19700.
16. **Gomez-Esquer, F., J. M. Rodriguez-Pena, G. Diaz, E. Rodriguez, P. Briza, C. Nombela, and J. Arroyo.** 2004. CRR1, a gene encoding a putative transglycosidase, is required for proper spore wall assembly in Saccharomyces cerevisiae. Microbiology **150:**3269–3280.
17. **Hopper, A. K., P. T. Magee, S. K. Welch, M. Friedman, and B. D. Hall.** 1974. Macromolecule synthesis and breakdown in relation to sporulation and meiosis in yeast. J. Bacteriol. **119:**619–628.
18. **Horton, R. M., H. D. Hunt, S. N. Ho, J. K. Pullen, and L. R. Pease.** 1989. Engineering hybrid genes without the use of restriction enzymes: gene splicing by overlap extension. Gene **77:**61–68.
19. **Kapteyn, J. C., R. C. Montijn, E. Vink, J. de la Cruz, A. Llobell, J. E. Douwes, H. Shimoi, P. N. Lipke, and F. M. Klis.** 1996. Retention of Saccharomyces cerevisiae cell wall proteins through a phosphodiester-linked beta-1,3-/beta-1,6-glucan heteropolymer. Glycobiology **6:**337–345.
20. **Kapteyn, J. C., B. ter Riet, E. Vink, S. Blad, H. De Nobel, H. Van Den Ende, and F. M. Klis.** 2001. Low external pH induces HOG1-dependent changes in the organization of the Saccharomyces cerevisiae cell wall. Mol. Microbiol. **39:**469–479.
21. **Klis, F. M., A. Boorsma, and P. W. De Groot.** 2006. Cell wall construction in Saccharomyces cerevisiae. Yeast **23:**185–202.
22. **Kollar, R., E. Petrakova, G. Ashwell, P. W. Robbins, and E. Cabib.** 1995. Architecture of the yeast cell wall. The linkage between chitin and beta(1→3)-glucan. J. Biol. Chem. **270:**1170–1178.
23. **Kollar, R., B. B. Reinhold, E. Petrakova, H. J. Yeh, G. Ashwell, J. Drgonova, J. C. Kapteyn, F. M. Klis, and E. Cabib.** 1997. Architecture of the yeast cell wall. Beta(1→6)-glucan interconnects mannoprotein, beta(→3)-glucan, and chitin. J. Biol. Chem. **272:**17762–17775.
24. **Kreger-Van Rij, N. J.** 1978. Electron microscopy of germinating ascospores of Saccharomyces cerevisiae. Arch. Microbiol. **117:**73–77.
25. **Lagorce, A., N. C. Hauser, D. Labourdette, C. Rodriguez, H. Martin-Yken, J. Arroyo, J. D. Hoheisel, and J. Francois.** 2003. Genome-wide analysis of the response to cell wall mutations in the yeast Saccharomyces cerevisiae. J. Biol. Chem. **278:**20345–20357.
26. **Leidich, S. D., and P. Orlean.** 1996. Gpi1, a Saccharomyces cerevisiae protein that participates in the first step in glycosylphosphatidylinositol anchor synthesis. J. Biol. Chem. **271:**27829–27837.
27. **Lesage, G., and H. Bussey.** 2006. Cell wall assembly in *Saccharomyces cerevisiae*. Microbiol. Mol. Biol Rev. **70:**317–343.
28. **Lesage, G., A. M. Sdicu, P. Menard, J. Shapiro, S. Hussein, and H. Bussey.** 2004. Analysis of beta-1,3-glucan assembly in Saccharomyces cerevisiae using a synthetic interaction network and altered sensitivity to caspofungin. Genetics **167:**35–49.
29. **Linding, R., R. B. Russell, V. Neduva, and T. J. Gibson.** 2003. GlobPlot: exploring protein sequences for globularity and disorder. Nucleic Acids Res. **31:**3701–3708.
30. **Livak, K. J., and T. D. Schmittgen.** 2001. Analysis of relative gene expression data using real-time quantitative PCR and the 2(-Delta Delta C(T)) Method. Methods **25:**402–408.
31. **Montijn, R. C., E. Vink, W. H. Müller, A. J. Verkleij, H. Van Den Ende, B. Henrissat, and F. M. Klis.** 1999. Localization of synthesis of β1,6-glucan in *Saccharomyces cerevisiae*. J. Bacteriol. **181:**7414–7420.
32. **Mouyna, I., T. Fontaine, M. Vai, M. Monod, W. A. Fonzi, M. Diaquin, L. Popolo, R. P. Hartland, and J. P. Latge.** 2000. Glycosylphosphatidylinositol-anchored glucanosyltransferases play an active role in the biosynthesis of the fungal cell wall. J. Biol. Chem. **275:**14882–14889.
33. **Neiman, A. M.** 2005. Ascospore formation in the yeast *Saccharomyces cerevisiae*. Microbiol. Mol. Biol. Rev. **69:**565–584.
34. **Popolo, L., P. Cavadini, M. Vai, and L. Alberghina.** 1993. Transcript accumulation of the GGP1 gene, encoding a yeast GPI-anchored glycoprotein, is inhibited during arrest in the G1 phase and during sporulation. Curr. Genet. **24:**382–387.
35. **Popolo, L., D. Gilardelli, P. Bonfante, and M. Vai.** 1997. Increase in chitin as an essential response to defects in assembly of cell wall polymers in the *ggp1*Δ mutant of *Saccharomyces cerevisiae*. J. Bacteriol. **179:**463–469.
36. **Popolo, L., T. Gualtieri, and E. Ragni.** 2001. The yeast cell-wall salvage pathway. Med. Mycol. **39**(Suppl.)**:**111–121.
37. **Popolo, L., and M. Vai.** 1999. The Gas1 glycoprotein, a putative wall polymer cross-linker. Biochim. Biophys. Acta **1426:**385–400.
38. **Primig, M., R. M. Williams, E. A. Winzeler, G. G. Tevzadze, A. R. Conway, S. Y. Hwang, R. W. Davis, and R. E. Esposito.** 2000. The core meiotic transcriptome in budding yeasts. Nat. Genet. **26:**415–423.
39. **Ram, A. F., J. C. Kapteyn, R. C. Montijn, L. H. Caro, J. E. Douwes, W. Baginsky, P. Mazur, H. van den Ende, and F. M. Klis.** 1998. Loss of the plasma membrane-bound protein Gas1p in *Saccharomyces cerevisiae* results in the release of β1,3-glucan into the medium and induces a compensation mechanism to ensure cell wall integrity. J. Bacteriol. **180:**1418–1424.

40. **Sanz, M., J. A. Trilla, A. Duran, and C. Roncero.** 2002. Control of chitin synthesis through Shc1p, a functional homologue of Chs4p specifically induced during sporulation. Mol. Microbiol. **43:**1183–1195.
41. **Shahinian, S., and H. Bussey.** 2000. Beta-1,6-glucan synthesis in Saccharomyces cerevisiae. Mol. Microbiol. **35:**477–489.
42. **Trew, B. J., J. D. Friesen, and P. B. Moens.** 1979. Two-dimensional protein patterns during growth and sporulation in *Saccharomyces cerevisiae*. J. Bacteriol. **138:**60–69.
43. **Vai, M., I. Orlandi, P. Cavadini, L. Alberghina, and L. Popolo.** 1996. Candida albicans homologue of GGP1/GAS1 gene is functional in Saccharomyces cerevisiae and contains the determinants for glycosylphosphatidylinositol attachment. Yeast **12:**361–368.
44. **Wyrick, J. J., F. C. Holstege, E. G. Jennings, H. C. Causton, D. Shore, M. Grunstein, E. S. Lander, and R. A. Young.** 1999. Chromosomal landscape of nucleosome-dependent gene expression and silencing in yeast. Nature **402:** 418–421.
45. **Yin, Q. Y., P. W. de Groot, H. L. Dekker, L. de Jong, F. M. Klis, and C. G. de Koster.** 2005. Comprehensive proteomic analysis of Saccharomyces cerevisiae cell walls: identification of proteins covalently attached via glycosylphosphatidylinositol remnants or mild alkali-sensitive linkages. J. Biol. Chem. **280:**20894–20901.
46. **Zlotnik, H., M. P. Fernandez, B. Bowers, and E. Cabib.** 1984. *Saccharomyces cerevisiae* mannoproteins form an external cell wall layer that determines wall porosity. J. Bacteriol. **159:**1018–1026.